

2023-02

Variability in feeding habitats of red deer sensu lato in Eurasia in the Late Pleistocene and Holocene

Sykut, M

<http://hdl.handle.net/10026.1/20205>

10.1016/j.jas.2023.105726

Journal of Archaeological Science

Elsevier BV

All content in PEARL is protected by copyright law. Author manuscripts are made available in accordance with publisher policies. Please cite only the published version using the details provided on the item record or document. In the absence of an open licence (e.g. Creative Commons), permissions for further reuse of content should be sought from the publisher or author.

1 **Variability in feeding habitats of red deer *sensu lato* in Eurasia in the Late Pleistocene and**
2 **Holocene**

3 Maciej Sykut^{a*}, Sławomira Pawełczyk^b, Natalia Piotrowska^b, Krzysztof Stefaniak^c, Bogdan
4 Ridush^d, Daniel Makowiecki^e, Pavel Kosintsev^{f,g}, Barbara Wilkens^h, Tomasz Borowik^a, Ralph
5 Fyfeⁱ, Jessie Woodbridgeⁱ, Magdalena Niedziałkowska^{a*}

6 * corresponding authors: msykut@ibs.bialowieza.pl; mniedz@ibs.bialowieza.pl

7 ^aMammal Research Institute, Polish Academy of Sciences, Stoczek 1c, 17-230 Białowieża, Poland

8 ^bDivision of Geochronology and Environmental Isotopes, Institute of Physics – CSE, Silesian
9 University of Technology, Konarskiego 22 B, 44-100 Gliwice, Poland.

10 ^cDepartment of Palaeozoology, University of Wrocław, Sienkiewicza 21, 50-335 Wrocław, Poland

11 ^dDepartment of Physical Geography, Geomorphology and Paleogeography, Yuriy Fedkovych
12 Chernivtsi National University, Kotsubynskogo 2, Chernivtsi 58012, Ukraine

13 ^eNicolaus Copernicus University, Institute of Archaeology, Department of Historical Sciences,
14 Szosa Bydgoska 44/48, 87-100 Toruń, Poland

15 ^fInstitute of Plant and Animal Ecology, Ural Branch of the Russian Academy of Sciences, 8 Marta
16 202, Yekaterinburg 620144, Russia

17 ^gUral Federal University, Prospekt Lenina, 51, Ekaterinburg, 620002, Russia

18 ^hIndependent researcher, Alghero, Italy

19 ⁱSchool of Geography, Earth and Environmental Sciences, University of Plymouth, Plymouth,
20 Devon PL4 8AA, UK

21 **Keywords: stable isotopes, carbon, nitrogen, *Cervus elaphus*, paleoecology, ungulates**

22 **Highlights**

- 23 • $\delta^{13}\text{C}$ and $\delta^{15}\text{N}$ values of ancient red deer and wapiti bones have been analysed
- 24 • We showed that $\delta^{13}\text{C}$ and $\delta^{15}\text{N}$ in deer fluctuated with environmental changes in Europe
- 25 • The values of $\delta^{13}\text{C}$ and $\delta^{15}\text{N}$ of red deer and wapiti overlapped
- 26 • Forest cover and July temperature influenced $\delta^{13}\text{C}$ values within Holocene deer bones
- 27 • Temperature, precipitation and altitude shaped $\delta^{15}\text{N}$ values within Holocene deer bones

28 **Abstract**

29 Red deer (*Cervus elaphus*) is one of the species that is rather wide spread and survived across
30 Europe over the Holocene. The analyses of carbon and nitrogen stable isotopes in bone collagen of
31 ungulate remains have been applied in paleoecological studies as environmental and dietary
32 indicators. In this study we present the carbon and nitrogen stable isotope compositions of
33 previously radiocarbon-dated red deer bone samples (N = 68) found in Central, Southern and
34 Eastern Europe and Asia and aligned to one of two species: European red deer (*Cervus elaphus*) and
35 wapiti (*Cervus canadensis*). We showed that the values of carbon and nitrogen stable isotope ratios
36 of European red deer and wapiti overlapped. Among all analyzed independent factors (determined
37 for the locality and time period relevant for each of the analysed samples), the variability of $\delta^{13}\text{C}$
38 values in European red deer dated to the Holocene is best explained by forest cover and mean July
39 temperature, and variability of $\delta^{15}\text{N}$ values by the mean July temperature, annual precipitation and
40 altitude. Additionally, combining the results of the present study with isotopic data on European red
41 deer collected from published sources, we revealed that the values of $\delta^{13}\text{C}$ and of $\delta^{15}\text{N}$ in *C. elaphus*
42 bones changed according to environmental oscillations that took place in Europe over the last
43 50 000 years. We concluded that red deer shifted their feeding habitats in relation to changing
44 environmental conditions, for example, forest expansion during the climate warming, and in the mid
45 to later Holocene in response to deforestation caused by human activity and the spread of
46 agriculture. We also found out that red deer reacted in varied ways to changing local conditions in

47 different regions of Europe. Modern individuals of *C. elaphus* had the lowest $\delta^{13}\text{C}$ values among all
48 analysed specimens, so they probably inhabited the most densely forested areas in comparison to
49 other European red deer populations during the last 50 000 years.

50 1. Introduction

51 Red deer (*Cervus elaphus*) *sensu lato* (*s.l.*) is one of the most widely distributed ungulate
52 species in the Holarctic (Geist, 1998; Milner *et al.*, 2006; Apollonio *et al.*, 2010). It probably
53 evolved in central Asia about 7 million years ago (mya) (Ludt *et al.*, 2004; Pitra *et al.*, 2004) during
54 the spread of grasses over large areas of Eurasia (Cerling *et al.*, 1997). In the late Early Pleistocene,
55 red deer *s.l.* appeared in southwestern Siberia (Alekseeva, 1980; Foronova, 1999, 2001) and during
56 the mid-Pleistocene in Europe (van der Made *et al.*, 2014; Stefaniak, 2015; van der Made &
57 Dimitrijević, 2015). About 15 000 years (15 ka) ago the species' range expanded to North America
58 via the Bering Strait (Meiri *et al.*, 2018).

59 In accordance with current taxonomic consensus, red deer *s.l.* comprises three species:
60 European/West Asian red deer (*C. elaphus* Linnaeus, 1758), Central Asian red deer (*C. hanglu*
61 Wagner, 1844) and East Asian/North American wapiti or elk (*C. canadensis* Erxleben, 1777)
62 (Lorenzini & Garofalo, 2015; Meiri *et al.*, 2018). Hereafter, the term red deer *s.l.* is used when we
63 refer to individuals of both species: red deer and wapiti, or we were unable to assign the individual
64 to particular species.

65 During the last 50 ka, the range of red deer *s.l.* changed in response to climate oscillations,
66 contracting during colder period and expanding during warmer episodes (Sommer *et al.*, 2008;
67 Meiri *et al.*, 2013; Doan *et al.*, 2022; Niedziałkowska *et al.*, 2021). In the Late Pleistocene (54.0 ka
68 – 34.0 ka before present (BP)), red deer *s.l.* occurred across almost the entire Europe from the
69 Atlantic coast to the Urals. Due to the climatic cooling (33.0 – 26.5 ka BP), the range of the species
70 shrunk reaching its minimum during the Last Glacial Maximum (LGM, 26.5 – 20.0 ka BP) (Clark
71 *et al.*, 2009). Within this time period, red deer *s.l.* are likely to have survived not only on the

72 Iberian, Apennine and Balkan Peninsulas (Skog *et al.*, 2009; Sommer & Zachos, 2009) but also, as
73 recent studies indicated, in western Europe, the Carpathians, surroundings of the Black Sea and the
74 Urals (Queiros *et al.*, 2019; Niedziałkowska *et al.*, 2021). After the LGM when the climate became
75 warmer, red deer *s.l.* populations recolonized the north and north-eastern parts of the continent
76 (Sommer *et al.*, 2008; Niedziałkowska *et al.*, 2021).

77 In the Late Pleistocene (between approximately 50 to 26 ka BP) the ranges of *C. elaphus*
78 (hereafter called “red deer”) and *C. canadensis* (hereafter called “wapiti”) partly overlapped in
79 southeastern Europe and in the Urals (Stankovic *et al.*, 2011; Meiri *et al.*, 2018; Doan *et al.*, 2022).
80 During this time, the wapiti inhabited vast areas of Eurasia from
81 present-day Romania to northeastern Asia until the LGM (Doan *et al.*, 2022) or for even longer
82 (Croitor & Obada, 2018). After the LGM, when the climate became warmer, their range moved to
83 the east and it was limited to Asia. During the last 4 ka BP, *C. canadensis* disappeared from the
84 Urals, western and northeastern Siberia (Doan *et al.*, 2022).

85 *Cervus elaphus* is a savanna-type deer with a mixed feeding strategy (Geist, 1998). Based on
86 mitochondrial DNA (mtDNA) studies four or five main haplogroups of extant red deer (called A-E)
87 have been identified (Ludt *et al.*, 2004; Skog *et al.*, 2009; Doan *et al.*, 2021). *Cervus canadensis* is a
88 more cold-adapted open-country grazer which inhabits dry, cold, continental regions (Geist, 1998).
89 Within wapiti, three main haplogroups (called X, Y and Z) have been described (Doan *et al.*, 2022).
90 Modern *C. elaphus* and *C. canadensis* inhabit geographically separate areas and their ecological
91 niches are slightly different (Geist, 1998; Brook *et al.*, 2018; Lovari *et al.*, 2018). In present time
92 red deer are widely distributed throughout most of Europe except northern Fennoscandia and large
93 areas of the European part of Russia (Lovari *et al.*, 2018). Modern wapiti occurs from the Tian-
94 Shan and the Altai Mountains to the Far East including mountainous areas and lowland boreal
95 forests (Stepanova, 2010; Brook *et al.*, 2018). Nowadays, due to climate warming, the wapiti has
96 been recolonizing eastern Siberia (Stepanova, 2010).

97 Since the Late Pleistocene red deer *s.l.* occurrence in Europe was mostly associated with
98 forest biomes (Niedziałkowska *et al.*, 2021). However, in the last 4 ka BP, the proportion of forests
99 in red deer habitats decreased significantly (Niedziałkowska *et al.*, 2021) as a result of human-
100 induced deforestation in Europe (Fyfe *et al.*, 2015; Roberts *et al.*, 2018). It is believed that forest is
101 the most suitable habitat for contemporary red deer (Borowik *et al.*, 2013), although both species:
102 red deer and wapiti occur in forest as well as in upland moors and open mountainous areas (Clutton-
103 Brock & Albon, 1989; Mattioli, 2011). Also studies of the Pleistocene specimens (described by the
104 authors as *C. elaphus*) from Western Europe showed that the species could have inhabited both
105 forested and open areas as well (Saarinen *et al.*, 2016). The diet of red deer *s.l.* in Europe (Gebert &
106 Verheyden-Tixier, 2001) and Asia (Chen *et al.*, 1998; Ohtsu & Takatsuki, 2021) may contain
107 eatable parts of tree and shrubs as well as grasses and sedges. According to analyses of diet of red
108 deer inhabiting different habitats in Europe, the main six major food items of the species were
109 Calluna and Vaccinium, conifers, twigs and bark, leaves of deciduous trees, Rubus, forbs, seeds and
110 fruits, which represented 59% of the diet. The variation in these food components was associated
111 with habitat types. The only food items, which differ seasonally were seeds and fruits. Grass and
112 sedges represented 29% of European red deer diet and their content did not varied between habitats
113 and seasons (Gebert & Verheyden-Tixier, 2001). Key plant species for *C. elaphus* in moorland were
114 Calluna and Vaccinium, in mixed-coniferous forests Calluna and Vaccinium and coniferous browse
115 and in mixed-deciduous forests fruits, leaves of deciduous trees and shrubs, twigs and bark (Gebert
116 & Verheyden-Tixier, 2001).

117 The analyses of carbon and nitrogen stable isotopes in bone collagen of ungulate remains
118 have been applied in paleoecological studies as environmental and dietary indicators (e.g. Drucker
119 *et al.*, 2003a; Drucker & Bocherens, 2009; Bocherens *et al.*, 2015). The isotope signatures of food
120 are transferred up the food chain to animals and are recorded in their tissues (Ambrose & Norr,
121 1993). However, carbon and nitrogen stable isotopic compositions of plants can be affected by
122 environmental factors (i.e. precipitation, temperature, salinity, altitude, forest cover) (Heaton, 1999;

123 Zhu *et al.*, 2010; Giroux *et al.*, 2015; Liu *et al.*, 2017). The combination of some of them leads to a
124 phenomenon known as “canopy effect”- change in $\delta^{13}\text{C}$ values along a vertical gradient of forest
125 trees and plants, with ^{13}C -enriched stable isotope values in the plants at the top of the canopy and
126 ^{13}C -depleted plants on the forest floor. The “canopy effect” is thereby reflected in lower $\delta^{13}\text{C}$ values
127 of plants growing under the canopy of dense forest stands compared with those grown in non-
128 forested habitats (e.g. Van der Merwe & Medina, 1991; Stevens *et al.*, 2004; Drucker *et al.*, 2008;
129 Bonafini *et al.*, 2013). The forest cover best explained the variability of $\delta^{13}\text{C}$ values in modern
130 ungulates such as red deer, European bison (*Bison bonasus*) and moose (*Alces alces*) as well as in
131 ancient cervids and large bovines (Drucker *et al.* 2008, Hofman-Kamińska *et al.*, 2018; Sykut *et al.*,
132 2021). Relatively low $\delta^{13}\text{C}$ values need to make us consider “canopy effect” and therefore, it is
133 possible to distinguish if the animals used to feed in forested or more open habitats (Drucker *et al.*,
134 2003a; Sykut *et al.*, 2021). Furthermore, $\delta^{15}\text{N}$ values also differ among groups of plants, for
135 instance, grasses, sedges, and forbs represent higher $\delta^{15}\text{N}$ values than shrubs and trees (Michelsen
136 1996, 1998; Amundson 2003). This allows grazing and browsing herbivore species to be
137 distinguished (Drucker *et al.*, 2003a). Additionally, studies of modern red deer showed that the
138 variability of $\delta^{15}\text{N}$ values of bone collagen are best explained by the percent of open area
139 representing their food source. This is due to the fact that open areas are covered by plants with a
140 higher $\delta^{15}\text{N}$ values e.g. grasses and thus $\delta^{15}\text{N}$ values can be also used as a proxy of habitat: closed
141 (forested) or more open habitats (Sykut *et al.*, 2021). The $\delta^{15}\text{N}$ values of plants are associated with
142 several different environmental factors such as local nitrogen soil pools, aridity levels, the mean
143 annual temperature (Stevens *et al.*, 2006; Drucker *et al.*, 2011; Bocherens *et al.*, 2014).

144 Based on the conclusions of the previous studies, we assume that the past feeding habitats of
145 red deer *s.l.* have been reflected in their bone collagen. As the range of the species changed in
146 response to climate oscillations, we hypothesize that habitats, where the individuals of red deer *s.l.*
147 used to forage, varied among different time periods and regions in Eurasia. We predict wapiti as
148 open country grazer represents lower $\delta^{13}\text{C}$ and higher $\delta^{15}\text{N}$ values than red deer – mixed feeder.

149 Despite the unequal number of analysed red deer and wapiti samples, we expect that the values of
150 $\delta^{13}\text{C}$ and $\delta^{15}\text{N}$ obtained for both deer lineages will not overlap. Due to the fact that the studied red
151 deer and wapiti belonged to several mtDNA haplogroups inhabited various geographic areas (comp.
152 Doan *et al.*, 2022), it is possible that they fed also in different habitats and various isotopic signals
153 will be obtained for individuals representing each of them. Furthermore, we hypothesise that
154 environmental variables such as percentage of forest cover, temperature, precipitation and altitude
155 will explain variability of $\delta^{13}\text{C}$ and $\delta^{15}\text{N}$ in European red deer during the Holocene. Finally, also
156 human induced large-scale deforestation of Europe during the last 4 ka BP (Fyfe *et al.*, 2015)
157 leading to red deer ecological niche transition can be reflected in changes of the isotopic
158 composition of their bone collagen. We expected the increase of $\delta^{13}\text{C}$ and decrease of $\delta^{15}\text{N}$ values
159 over that time period.

160 This paper seeks to: (a) reveal the feeding habitats of red deer in the Late Pleistocene and the
161 Holocene in Europe, (b) investigate whether these habitats varied in time and space and if there are
162 differences in $\delta^{13}\text{C}$ and $\delta^{15}\text{N}$ values among species and haplogroups within the species, (c) identify
163 environmental variables that best explain variance in $\delta^{13}\text{C}$ and $\delta^{15}\text{N}$ values in European red deer in
164 the Holocene.

165

166 **2. Materials and methods**

167 **2.1. Sampling**

168 Red deer (*s.l.*) subfossil fragments of bones were compiled from zoological and
169 archaeological collections in Europe and Asia in agreement with the collection owners. The ancient
170 sample set analysed in this study (N = 68, Tab. S1) covers northeastern Europe, the Carpathian
171 Mountains region, the Eastern Alps, Italy and Corsica and southeastern Europe as well as the Ural
172 Mountains, Eastern and Western Siberia from 41°W to 131° E (Fig. 1) and extends from the Late
173 Pleistocene (48 ka cal BP) until historical times (ca. 200 cal BP). Species identification was based
174 on comparative macroscopic and morphometric analyses and confirmed by sequencing of

175 cytochrome *b* of mitochondrial DNA (mtDNA), see Doan *et al.* (2017) for details. The results of
176 genetic analyses (1131 bp long fragments of cytochrome *b* sequences) allowed us to assign the
177 samples to one of two red deer species: European red deer (*Cervus elaphus*) and wapiti deer
178 (*Cervus canadensis*) and further *C. elaphus* specimens into mtDNA haplogroups A-F, and *C.*
179 *canadensis* specimens into mtDNA haplogroups X, Y and Z (Tab. S1; for more details see Doan *et*
180 *al.*, 2022).

181 The bone samples of red deer *s. l.* specimens were radiocarbon-dated using accelerator mass
182 spectrometry (AMS) at the Division of Geochronology and Environmental Isotopes at the Institute
183 of Physics, Silesian University of Technology (Gliwice, Poland). Dates used in this study have been
184 published by Niedziałkowska *et al.* (2021) (50 samples), Doan *et al.* (2022) (10 samples), and Doan
185 *et al.* (2017) (8 samples) (Tab. S1).

186 The literature searches were performed to include into the analyses additional isotopic data
187 of red deer specimens dated to the Late Pleistocene and the Holocene from other regions of Europe:
188 the Cantabria Mountains in Spain (Castaños *et al.*, 2014; Stevens *et al.*, 2014; Rofes *et al.*, 2015;
189 Jones *et al.*, 2018, 2019, 2020), southwestern France (Bocherens *et al.*, 2014), northern France
190 (Drucker *et al.*, 2020), the French Jura (Drucker *et al.*, 2011), the Western Alps in France (Drucker
191 *et al.*, 2011), Sicily and southern Italy (Craig *et al.*, 2010; Mannino *et al.*, 2011a, 2011b; Di Maida
192 *et al.*, 2019), (Fig. 1, Tab. S2). Data from the literature was generated using key word searches
193 (“*stable isotope*” and “*deer*”) in the Web of Science (Clarivate Analytics). We used records that
194 have been radiocarbon-dated either directly or indirectly, i.e. dates derived from charcoal, humus or
195 bones of other animals found in the same layer as red deer fossils. We did not include in our
196 analyses localities, with less than 10 red deer records. Samples from the literature without
197 radiocarbon-dates or without given collagen quality criteria (%C, %N, C/N ratio) were excluded
198 from the analysis.

199 Stable isotopic data of modern European red deer samples were taken from Sykut *et al.*,
200 (2021). We randomly selected 49 samples (Tab. S3) from the entire set of modern samples ($n =$

201 242). The number of modern samples has been matched, so that they were not overrepresented in
202 the whole data set. These samples were collected from various habitats in Poland, Scotland, the
203 Netherlands and Slovenia: (1) large woodlands, (2) mosaic of meadows, arable grounds and forest
204 areas, and (3) grasslands (Fig. S1). The details concerning those habitats has been described in
205 S1Table in Sykut *et al.* (2021). Due to anthropogenic CO₂ emissions, the $\delta^{13}\text{C}$ values of modern
206 samples have been corrected for the shift in $\delta^{13}\text{C}$ values according to the formula proposed by Feng
207 (1998) and provided in Sykut *et al.*, (2021).

208 All radiocarbon dates (obtained in the frame of this study and from the literature) were
209 calibrated using OxCal v. 4.2 (Bronk Ramsey, 2009) and the IntCal20 calibration curve (Reimer *et*
210 *al.*, 2020). Hereafter, the dates are provided as cal BP, i.e. calibrated age in years before AD 1950,
211 using medians of the calibrated ages.

212 **2.2. Sample preparation and analysis**

213 The collected bone samples (approximately 1 g) were cleaned in an ultrasonic bath in
214 demineralized water, then dried and ground in a ball mill. The powdered bone was demineralized in
215 0.5 M hydrochloric acid at room temperature in a glass vial. The acid was replaced several times,
216 and the reaction was considered complete when pH stabilized at < 1 and no bubbles were observed.
217 The insoluble residue was rinsed with demineralized water to neutral pH (Piotrowska & Goslar,
218 2002). The bone collagen was extracted according to the classical Longin method (Longin, 1971)
219 with modification applied in the Gliwice Radiocarbon Laboratory (Piotrowska & Goslar, 2002).
220 Gelatinization was performed as follows: the residue was acidified and maintained at 80°C for 12 hr
221 in an acidic solution (HCl, pH = 3). The obtained supernatant was centrifuged, transferred to a glass
222 vial and dried in an oven at 75°C. The subsample of gelatin was subjected to graphite preparation
223 using an AGE-3 system equipped with a VarioMicroCube by elemental analyzer and automated
224 graphitization unit (Němec *et al.*, 2010; Wacker *et al.*, 2010). The ¹⁴C concentrations in graphite
225 produced from blank samples, Oxalic Acid II standards, and coal blanks have been measured by the
226 Direct AMS laboratory, Bothell, USA (Zoppi *et al.*, 2007; Zoppi, 2010). Another gelatin subsample

227 was assigned for analysis of carbon and nitrogen stable isotope composition ($\delta^{13}\text{C}$, $\delta^{15}\text{N}$), %C, %N,
228 and C/N_{at}. The dried collagen was weighed into tin capsules. Three subsamples of each collagen
229 sample were prepared for the measurements. The elemental and isotopic measurements were
230 performed at the Division of Geochronology and Environmental Isotopes at the Institute of Physics,
231 Silesian University of Technology (Gliwice, Poland) using an IsoPrime EA-CF-IRMS continuous
232 flow isotope ratio mass spectrometer connected to the EuroVector elemental analyser. The obtained
233 carbon and nitrogen isotope measurements were calibrated to VPDB and AIR standards,
234 respectively (Coplen *et al.* 2006, Mariotti 1983). The stable isotope values were expressed in the
235 isotope delta (δ) notation as follows:

236
237 ‰)
238
239 and
240
241 ‰)

242
243
244 The $\delta^{13}\text{C}$ and $\delta^{15}\text{N}$ values are presented in units of part per thousand and communicated in
245 per mil shown as ‰ (Brand & Coplen, 2012). Samples of collagen were routinely calibrated to
246 international standards. The $\delta^{13}\text{C}$ values were calibrated to values of IAEA-C8 ($\delta^{13}\text{C} = -18.31\text{‰}$)
247 and IAEA-C5 ($\delta^{13}\text{C} = -25.49\text{‰}$). The $\delta^{15}\text{N}$ values are calibrated to values of IAEA-NO3 ($\delta^{15}\text{N} =$
248 4.7‰) and IAEA-USGS34 ($\delta^{15}\text{N} = -1.8\text{‰}$). C/N elemental ratio values were calibrated to values of
249 UREA (elemental composition: C – 20%, H – 6,71%, N – 46,65% and O – 26,64%). The precision
250 of these methods is lower or equal to 0.1‰ for $\delta^{13}\text{C}$ and 0.2‰ for $\delta^{15}\text{N}$. Samples with quality
251 collagen extracts similar to those obtained from fresh bone (%C > 10, %N > 3, $2.9 \leq \text{C/N} \leq 3.6$)
252 were considered a reliable source of isotopic signatures (DeNiro, 1985; Ambrose, 1990) and were
253 used for further analyses. For samples with atomic C/N ratios above 3.6, which may indicate
254 extraneous carbon contamination from humin acids, we applied NaOH treatment and ultrafiltration
255 and again tested the collagen quality.

256 **2.3. Climatic and environmental analyses**

257 The climatic and biome data for each of the analysed samples have been taken from
258 Niedziałkowska *et al.* (2021) and are presented in Table S1. These data (mean annual, mean
259 January, mean July temperatures, annual, January and July precipitation, biome) were obtained
260 from the FAMOUS database (FAst Met. Office and UK Universities Simulator) available online
261 (Smith & Gregory, 2012) as described in Niedziałkowska *et al.* (2021). For the requirements of
262 statistical analyses (to have enough number of samples in different biome categories), we merged
263 the biomes from FAMOUS database into the four following categories: Forest (Cool conifer,
264 Deciduous taiga/montane and Warm mixed forest), Mixed (Temperate xerophytic shrub and
265 Temperate sclerophyll woodland), Open (Steppe tundra, Shrub tundra and Prostrate shrub tundra)
266 and Desert.

267 Information on the relative proportion of forest cover in the European sites, where the deer
268 samples dated to the Holocene (11– 0 ka BP) were recorded, was obtained from a pollen-inferred
269 land cover change database after Fyfe *et al.* (2015) and the values for each of the studied samples
270 have been taken from Niedziałkowska *et al.* (2021). This database contains pan-European land
271 cover classification for the last 11 ka BP years at 200-year temporal resolution and was created as
272 described in Niedziałkowska *et al.* (2021). The proportion of forest cover for modern sample
273 locations was estimated as described in Sykut *et al.* (2021) based on CORINE Land Cover maps
274 using ArcGIS 10.3.1 (ESRI, 2015) software.

275 **2.4. Statistical analyses**

276 The entire data set was divided based on the age of the samples: before the LGM and after
277 the LGM (the Holocene) due to significantly different environmental and climatic conditions during
278 these two periods (Markova *et al.*, 2008). Samples dated to the period before the LGM (47 857 – 26
279 813 cal BP) were genetically assigned to wapiti deer (n = 16) and European red deer (n = 4). The
280 sample set dated to the period after the LGM (9 508 – 189 cal BP) consisted mainly of European
281 red deer (n = 48) and only three samples were assigned to wapiti deer.

282 We tested the relationship between isotopic composition ($\delta^{13}\text{C}$, $\delta^{15}\text{N}$) and the age of the
283 samples separately for the two time periods (before and after the LGM) using Pearson correlation.
284 Due to low sample numbers and the different ecological niches of the two deer species (Geist,
285 1998), we excluded European red deer from the statistical analyses of samples dated to the time
286 period before the LGM and wapiti deer from the analyses of samples dated to the period after the
287 LGM.

288 To analyze changes in $\delta^{13}\text{C}$ and $\delta^{15}\text{N}$ values in *C. elaphus* bones during the last 50 ka cal
289 BP, we combined isotopic data presented in this study with the literature data on ancient and
290 modern European red deer. Data obtained in this study ($n = 49$) were divided according to the
291 regions where the analysed ancient sample were recorded as follows: the Carpathian Mountains
292 region ($n = 12$), the southeastern Europe ($n = 14$), the northeastern Europe ($n = 14$), Italy (including
293 Sardinia) and Corsica ($n = 8$) and the Eastern Alps ($n = 1$), (Tab. S1). The data on ancient samples
294 from the literature ($n = 440$) were divided as follows: the Cantabria Mountains ($n = 292$), the
295 French Jura ($n = 61$), the Western Alps ($n = 19$), northern France ($n = 13$), southwestern France ($n =$
296 30) and Sicily and southern Italy ($n = 25$) (Tab. S2). For each of the regions, except the Eastern
297 Alps (only one sample), we checked with regression analysis if $\delta^{13}\text{C}$ and $\delta^{15}\text{N}$ values of ancient
298 samples had been significantly changing over time.

299 Furthermore, we used GAM (Generalized Additive Model) analysis to illustrate how the
300 $\delta^{13}\text{C}$ and $\delta^{15}\text{N}$ values have been changing during the last 50 ka cal BP in all studied individuals of
301 European red deer (ancient and modern) treated as one group. The GAM analyses were performed
302 using the *mgcv* package (Wood, 2017) implemented in R version 4.0.2 (R Development Core Team,
303 2018).

304 The relationship between $\delta^{13}\text{C}$ and $\delta^{15}\text{N}$ and forest cover was analyzed separately for 41
305 ancient samples dated to the Holocene (9508 – 189 cal BP) (Tab. S4) and 49 modern samples (Tab.
306 S3) in R version 4.0.2 (R Development Core Team, 2018).

307 Normal linear models (NLM) with a Gaussian error structure were used to test associations
308 between the stable isotope composition ($\delta^{13}\text{C}$ or $\delta^{15}\text{N}$) of 39 European red deer samples dated to the
309 Holocene (9508 – 189 cal BP) and the following variables: median of calibrated age BP (hereafter
310 called median cal BP), mtDNA haplogroup of the analysed samples, annual mean temperature,
311 January mean temperature, July mean temperature, annual precipitation, January precipitation, July
312 precipitation, altitude, biome, percentage of forest cover, where the analysed samples were recorded
313 in certain time periods. Longitude and latitude were not included in the set of variables due to the
314 low informative value of including this information and high autocorrelation with other
315 environmental variables (Tab. S5). The median calibrated age BP of samples was included as a
316 covariate to correct for the effect of the time period on the results of modelling. Due to the low
317 number of samples each model consisted of one variable and the covariate. The homoscedasticity in
318 distribution of final model residuals was checked by visual inspection of plots presenting model
319 residuals against fitted values (estimated responses). Due to the lack of forest cover data for the
320 samples dated to the Late Pleistocene, these samples were not included in these analyses. We also
321 excluded the only red deer sample assigned to the mtDNA haplogroup D from these analyses due to
322 the lack of group equality. We ran separate models with $\delta^{13}\text{C}$ and $\delta^{15}\text{N}$ values as the response
323 variables. All LM models were performed using the *lmerTest* package (Kuznetsova *et al.*, 2015)
324 implemented in R version 4.0.2 (R Development Core Team, 2018).

325 To test which set of variables best explained the observed variance in $\delta^{13}\text{C}$ and $\delta^{15}\text{N}$ values,
326 we created two sets (one for $\delta^{13}\text{C}$ and one for $\delta^{15}\text{N}$) of competing models. Next, the competing
327 models were ranked with the Akaike Information Criterion (AIC) with the second-order correction
328 for a small sample size (AICc) (Burnham & Anderson, 2002) using the *MuMin* package (Bartoń,
329 2013) implemented in R version 4.0.2 (R Development Core Team, 2018). All models close to the
330 top performing model (lowest AICc), having $\Delta\text{AIC} < 2$, were considered to have substantial
331 empirical support. For the top models (or equal to the top) we created plots using the *effect* package
332 (Fox & Weisberg, 2019) implemented in R version 4.0.2 (R Development Core Team, 2018).

333

334 **3. Results**

335 **Variability of $\delta^{13}\text{C}$ and $\delta^{15}\text{N}$ in wapiti and red deer before the LGM**

336 The set of samples within this study dated to the period before the LGM comprised of
337 European red deer bones ($n = 4$) from Central and Southern Europe (from 19° to 34° E) and wapiti
338 deer bones ($n = 16$) from Eastern Europe and Asia (from 52° to 131° E). The median age of the
339 samples ranged from 47 857 to 26 813 cal BP. The values of $\delta^{13}\text{C}$ ranged from
340 -21.2 to -18.6‰ , and $\delta^{15}\text{N}$ from 4.5 to 10.3‰ (Fig.2 upper and lower panels). Due to the low
341 number of European red deer samples dated to the period before the LGM, the correlation between
342 $\delta^{13}\text{C}$, $\delta^{15}\text{N}$ and the median cal age of these samples were not tested. In wapiti samples no correlation
343 of sample age (median cal BP) was observed with either $\delta^{13}\text{C}$ or $\delta^{15}\text{N}$ (Fig. 2 upper and lower
344 panels). There was also no relationship between $\delta^{13}\text{C}$ and $\delta^{15}\text{N}$ values (Fig. S2 upper panel). The
345 range of $\delta^{13}\text{C}$ and $\delta^{15}\text{N}$ values (-21.2 to -18.6‰ and 4.5 to 10.3‰ respectively) obtained from
346 samples from the forest biome ($n = 8$) overlapped with the range of values obtained from samples
347 from open ($n = 7$) and mixed biomes ($n = 1$) (Fig. S2 upper panel). Additionally, the values of $\delta^{13}\text{C}$
348 and $\delta^{15}\text{N}$ of red deer samples from mixed ($n = 1$) and forest ($n = 3$) biomes were in the range of
349 these values for wapiti deer (Fig. 2 upper and lower panels).

350 **Variability of $\delta^{13}\text{C}$ and $\delta^{15}\text{N}$ in European red deer and wapiti in the Holocene**

351 The set of samples dated to the period after the LGM (the Holocene) comprised of European
352 red deer bones ($n = 45$) from Central and Southern Europe (from 8° to 48° E) and wapiti bones ($n =$
353 3) from Asia (from 60° to 105° E). The median age of the samples ranged from 9508 to 189 cal BP.
354 The values of $\delta^{13}\text{C}$ ranged from -23.3 to -19.3‰ , and $\delta^{15}\text{N}$ from 2.9 to 10.6‰ , (Fig. 3 upper and
355 lower panels). In the case of the European red deer samples, no correlation was observed between
356 $\delta^{13}\text{C}$ and the age of the samples (median cal years BP) (Fig. 3 upper panel), while the correlation
357 between $\delta^{15}\text{N}$ and the age of the samples (median cal BP) was positive and statistically significant (r
358 $= 0.5$, $p < 0.001$, Fig. 3 lower panel). The $\delta^{15}\text{N}$ values decreased with the median age. The

359 correlation between $\delta^{13}\text{C}$ and $\delta^{15}\text{N}$ values of red deer samples was positive and statistically
360 significant ($r = 0.35$, $p = 0.02$, Fig. S2 lower panel). Due to the low number of wapiti samples dated
361 after the LGM, the correlations between $\delta^{13}\text{C}$, $\delta^{15}\text{N}$ and age were not tested. The range of $\delta^{13}\text{C}$ and
362 $\delta^{15}\text{N}$ values (-23.2 to -19.3‰ and 2.9 to 10.6‰ respectively) of samples from the forest biome ($n =$
363 35) overlapped with the ranges of values obtained from red deer inhabiting the mixed biome ($n =$
364 10). Additionally, the values of $\delta^{13}\text{C}$ and $\delta^{15}\text{N}$ of wapiti samples from the forest biome ($n = 3$) were
365 in the range of values obtained for red deer (Fig. 3 upper and lower panels).

366 **Chronological changes in $\delta^{13}\text{C}$ and $\delta^{15}\text{N}$ of the European red deer bones during the last 50 ka** 367 **cal BP**

368 The relationship between $\delta^{13}\text{C}$ and $\delta^{15}\text{N}$ values and the median age of European red deer
369 samples (data sets from other studies are also included) varied depending on locality and time.
370 Among the isotopic results, the $\delta^{13}\text{C}$ values of samples from Cantabria (dated to 49.2 – 4.0 ka cal
371 BP), northern France (11.4 – 5.0 ka cal BP), the French Jura (14.2 – 6.8 ka cal BP), and Italy and
372 Corsica (9.5 – 0.6 ka cal BP) were positively correlated with median age (Tab. S6). The $\delta^{13}\text{C}$ values
373 decreased from older to more recent time periods (Fig. 4 upper panel).

374 The $\delta^{15}\text{N}$ values of samples from Cantabria (49.2 – 4.0 ka cal BP) and the Carpathian
375 Mountains region (6.0 – 0.2 ka cal BP) were positively correlated with median age and higher
376 values were recorded for samples dated to the older time periods (Fig. 4 lower panel, Tab. S6).
377 Negative correlations were recorded between $\delta^{15}\text{N}$ values and the median age of samples from
378 northern France (11.4 – 5.0 cal BP), the French Jura (14.2 – 6.8 ka cal BP) and Sicily and southern
379 Italy (18.5 – 9.3 ka cal BP). The $\delta^{15}\text{N}$ values of samples increased between older and younger time
380 periods (Fig. 4 lower panel, Tab. S6).

381 The $\delta^{13}\text{C}$ values of the European deer samples (all data sets pooled together) dated to the
382 period from about 50.0 to 14.0 ka cal BP oscillated mostly between -20 and -21‰. Over this time
383 period, mean $\delta^{13}\text{C}$ value hardly changed. Between 14.0 and 7.7 ka cal BP $\delta^{13}\text{C}$ mean value
384 decreased from -20.4 to -21.7‰. Over the period from 7.7 to 5.3 ka cal BP, mean $\delta^{13}\text{C}$ value hardly

385 changed and from 5.3 ka cal BP until modern times decreased from -21.7‰ to
386 -22.4‰ (Fig. 5 upper panel, Tables S1–S3).

387 The $\delta^{15}\text{N}$ values of the European deer samples (all data sets pooled together) for the period
388 from about 50.0 to 33.0 ka cal BP varied and ranged between 9.2 and 1.0‰. However, over this
389 period mean $\delta^{15}\text{N}$ value hardly changed. Between 33.0 and 15.5 ka cal BP the mean $\delta^{15}\text{N}$ value
390 decreased from 5.1 to 3.0‰. From 15.5 to 6.0 ka cal BP mean $\delta^{15}\text{N}$ values increased from 3.0 to
391 5.6‰. Over the period from 6.0 to modern times the mean $\delta^{15}\text{N}$ value decreased from 5.6 to 4.0‰
392 (Fig. 5 lower panel, Tables S1–S3).

393 **The influence of forest cover on $\delta^{13}\text{C}$ and $\delta^{15}\text{N}$ values in ancient and modern samples**

394 Forest cover in localities of the Holocene European red deer samples from this study ranged
395 from 31 to 80%, and for modern samples from 0 to 100% (Tables S1, S3). The values of $\delta^{13}\text{C}$ and
396 $\delta^{15}\text{N}$ within Holocene samples ranged from -23.3‰ to -19.3‰ and from 2.9‰ to 10.6‰,
397 respectively. The values of $\delta^{13}\text{C}$ and $\delta^{15}\text{N}$ of modern samples ranged from -24.1‰ to -20.9‰ and
398 from 0.6‰ to 8.5‰, respectively. The percentage of forest cover was negatively associated with
399 $\delta^{13}\text{C}$ values in both modern and ancient samples ($r = -0.54$, $p = 0.002$, and $r = -0.49$, $p = 0.001$,
400 respectively) (Fig. 6 upper panel). The percentage of forest cover was not associated with $\delta^{15}\text{N}$ in
401 ancient samples ($r = 0.01$, $p = 0.96$), while in modern samples a significant negative relationship
402 was observed ($r = -0.56$, $p = 0.001$) (Fig. 6 lower panel).

403 **Environmental factors explaining the variability of $\delta^{13}\text{C}$ and $\delta^{15}\text{N}$ in European red deer in the** 404 **Holocene**

405 Modeling was performed using the 39 Holocene *C. elaphus* samples (9.5 – 0.2 ka cal BP)
406 from Europe obtained in this study. Based on the AICc criteria, the best models explaining variation
407 in $\delta^{13}\text{C}$ values in bone collagen of red deer were the top-ranked models, which consisted of the
408 following variables – (i) median age and percentage of forest cover, (ii) median age and July
409 temperature (Tab. 1). The $\delta^{13}\text{C}$ values were negatively associated with forest cover percentage
410 (slope = -3.59 ± 0.93 , $t = -3.85$, $p < 0.001$). With increasing percentage forest cover from 31 to

411 80%, $\delta^{13}\text{C}$ values decreased from -20.9‰ to -22.6‰ (Fig. 7, upper panel). The $\delta^{13}\text{C}$ values were
412 positively associated with mean July temperature (slope = 1.38 ± 3.56 , $t = 3.87$, $p < 0.001$). With
413 increasing mean July temperature from ca. 10 to 26°C, $\delta^{13}\text{C}$ values increased from -23.0‰ to -
414 20.8‰ (Fig. 7, lower panel). Percentage of forest cover was negatively correlated with mean July
415 temperature ($r = -0.80$, $p < 0.05$) (Tab. S5).

416 Based on the AICc criteria, the best models explaining variation in $\delta^{15}\text{N}$ values in bone
417 collagen of red deer were the top-ranked models, which consisted of the following variables
418 – (i) median age and mean July temperature, (ii) median age and annual precipitation, (iii) median
419 age and altitude, (iv) median age and mean July precipitation, (v) median age and mean annual
420 temperature (Tab. 2). However, models (iv) and (v) were not statistically significant ($p = 0.125$ and
421 $p = 0.129$ respectively). The $\delta^{15}\text{N}$ values were positively associated with mean July temperature
422 (slope = 0.12 ± 0.06 , $t = 2.07$, $p = 0.046$). With increasing mean July temperature from ca. 10 to
423 26°C, $\delta^{15}\text{N}$ values increased from 4.1‰ to 5.9‰ (Fig. 8, upper panel). The $\delta^{15}\text{N}$ values were
424 negatively associated with the annual precipitation (slope = -0.002 ± 0.001 , $t = -2.01$, $p = 0.052$).
425 With increasing annual precipitation from ca. 450 to 1500 mm, $\delta^{15}\text{N}$ values decreased from 5.7‰ to
426 3.5‰ (Fig. 8, upper panel). The $\delta^{15}\text{N}$ values tended to be negatively associated with the altitude
427 (slope = -0.001 ± 0.001 , $t = -1.78$, $p = 0.084$). With increasing altitude from ca. -100 to 1650 m,
428 $\delta^{15}\text{N}$ values decreased from 5.6‰ to 3.6‰ (Fig. 8, lower panel). The decrease in $\delta^{15}\text{N}$ values per
429 1000 m amounted c. 1.14‰. Annual precipitation is negatively correlated with mean July
430 temperature ($r = -0.62$, $p < 0.05$) and positively correlated with altitude ($r = 0.53$, $p < 0.05$) (Tab.
431 S5). Mean July temperature is negatively correlated with altitude ($r = -0.26$, $p < 0.05$) (Tab. S5).

432

433 **4. Discussion**

434 Within the results of isotopic analyses of red deer samples from the present study and
435 available in the literature, dated from 50.0 to 14.0 ka cal BP, $\delta^{13}\text{C}$ values were no lower than
436 -22.5‰. Values lower than -22.5‰ can indicate the presence of the ‘canopy effect’ as indicated in

437 studies of ungulates inhabiting temperal and boreal ecosystems (Drucker *et al.*, 2008; Bocherens *et*
438 *al.*, 2015, Sykut *et al.* 2021). So the obtained results revealed that during this time period the
439 analysed individuals mainly fed on plants growing in more open habitats. However, the set of
440 samples from this long period mostly came from the Cantabria region (Spain) and Southwestern
441 France. Low variability of $\delta^{13}\text{C}$ values throughout this period indicate a lack of extreme changes in
442 climate and vegetation in this region (Jones & Britton, 2019). A decrease in $\delta^{13}\text{C}$ values in the
443 following postglacial period (14.0 – 6.4 ka cal BP) most likely corresponded to a climate-induced
444 (Sommer, 2020) habitat shift from open or mixed areas to closed and densely forested habitats
445 (Drucker *et al.*, 2011). Such decrease of $\delta^{13}\text{C}$ values in this time period was indicated also in local
446 populations (Fig. 4) e.g. in red deer inhabiting French Jura, (Drucker *et al.*, 2003a) and the Northern
447 France (Drucker *et al.*, 2020). It is in agreement with larger scale studies which indicated that red
448 deer (*s.l.*) in Europe and the Urals inhabited open and mixed areas during the Late Pleistocene,
449 while during the Holocene their habitats shifted from open and mixed areas to forests
450 (Niedziałkowska *et al.*, 2021). The lowest values in this postglacial period were observed during the
451 Holocene climatic optimum, which is coherent with the greatest extent of forested areas dated
452 between 8.5 and 6.0 ka cal BP (Zanon *et al.*, 2018). After the Holocene climatic optimum, an
453 increase in human activity was observed (Puhe & Ulrich, 2001; Gignoux *et al.*, 2011). A slight
454 increase in red deer $\delta^{13}\text{C}$ values during the period from 6.4 to 3.6 ka cal BP may reflect
455 environmental changes induced by the development of agriculture and demographic expansion at
456 that time (Puhe & Ulrich, 2001). Archaeological studies revealed that agricultural practices and
457 further population growth spread quickly across the Mediterranean regions of Europe (Gignoux *et*
458 *al.*, 2011). The development of agriculture and demographic expansion resulted in increasing
459 deforestation of European landscapes (Anderson *et al.*, 2007; Marquer *et al.*, 2017; Roberts *et al.*,
460 2018). In the last analysed period (from 3.6 ka cal BP to modern times) further decline in red deer
461 $\delta^{13}\text{C}$ values was observed. In this time period deforestation of Europe, associated with human
462 activities, intensified (Fyfe *et al.*, 2015). The observed decrease in $\delta^{13}\text{C}$ values of red deer bones can

463 be explained by a shift of the species' habitat to more forested areas to avoid human pressure
464 related to the spread of agriculture and increasing hunting activity (Lone *et al.*, 2015; Dixon *et al.*,
465 2021). A similar pattern of $\delta^{13}\text{C}$ changes were observed in the Holocene in other large ungulate
466 species, such as the European bison, aurochs (*Bos primigenius*), European moose (Hofman-
467 Kamińska *et al.*, 2019) and horse (*Equus ferus* and *Equus caballus*) (Stevens & Hedges 2004).
468 However, the explanation of those changes has been under debated. Stevens & Hedges (2004)
469 believed the faunal $\delta^{13}\text{C}$ mainly reflected changing plant $\delta^{13}\text{C}$ values due to an increase in
470 atmospheric CO_2 concentration, while Hofman-Kamińska *et al.* (2019) argued that variation of $\delta^{13}\text{C}$
471 values corresponded to a shift in foraging habitats and diet of large herbivores. The $\delta^{13}\text{C}$ values in
472 bones of contemporary red deer are generally lower among those dated to earlier time periods.
473 Modern red deer populations have probably inhabited the most densely forested areas in
474 comparison to populations of this species living in Europe over the last 50 ka. Nowadays red deer
475 may inhabit forest as a 'refuge areas' more often than before to avoid increasing human pressure, as
476 it was indicated for other large ungulate species occurring in contemporary times e.g. European
477 bison (Kerley *et al.*, 2012).

478 As more factors influence bone nitrogen than carbon isotopic composition, we observed
479 higher variability in $\delta^{15}\text{N}$ values than $\delta^{13}\text{C}$ values in red deer bones during the last 50 ka cal BP.
480 Temperature, aridity, soil maturity, distance to the sea or type of consumed plants are the
481 parameters that drive significant changes in $\delta^{15}\text{N}$ values in herbivores (e.g. Iacumin *et al.*, 2000;
482 Drucker *et al.*, 2003a; Sykut *et al.*, 2021). The $\delta^{15}\text{N}$ values of red deer samples dated between
483 50 and 40 ka cal BP mostly from Cantabria region indicated, in agreement with the results of pollen
484 based analyses (Jones & Britton, 2019 and references therein) and carbon isotopic composition
485 analyses (this study), that the studied individuals used to feed in open steppe areas. An increase in
486 $\delta^{15}\text{N}$ values during the following period, with the maximum values obtained for samples dated to
487 about 40 – 35 ka cal BP, was observed in red deer from Cantabria and southwestern France as well
488 as in other large ungulate species such as reindeer (*Rangifer tarandus*), large bovine (*Bos*

489 *primigenius* or *Bison priscus*), and horse (*Equus ferus*) inhabiting southwestern France (Bocherens
490 *et al.*, 2014). The ^{15}N enrichment in samples from this period is interpreted as a consequence of
491 increasing aridity (Bocherens *et al.*, 2014). Subsequently, a significant decrease of red deer $\delta^{15}\text{N}$
492 values was observed after 26 ka cal BP, reaching the lowest values during the LGM. A similar
493 pattern was observed in horse and reindeer from southwestern France (Drucker *et al.*, 2003b) and
494 Switzerland (Reade *et al.*, 2020) at this time associated with the combination of prolonged low
495 temperatures, limited bioavailable soil nutrients, and elevated nutrient demand from increasing
496 vegetation cover. In contrast to southwestern France and Switzerland, collagen of red deer from
497 Sicily and Southern Italy exhibited increase in $\delta^{15}\text{N}$ values during the LGM. This increase was
498 linked with arid conditions (Drucker *et al.*, 2003b). The significant increase in $\delta^{15}\text{N}$ values of deer
499 collagen was observed during warmer episodes over postglacial times and the early Holocene. This
500 may be explained by the effects of increased mean annual temperature (Davis *et al.*, 2003) on soil
501 development, intense nitrogen turnover and to ^{15}N enrichment in soils and plants (Drucker *et al.*,
502 2003a). This trend was not observed in red deer from Cantabria region, which could indicate a lack
503 of extreme changes in climate and vegetation in this region (Jones *et al.*, 2020). In the most recent
504 period analysed (from 8 ka cal BP to modern) a significant decline in $\delta^{15}\text{N}$ values was observed.
505 During this period human induced environmental changes occurred (i.e. agriculture development
506 and deforestation). The decline in red deer $\delta^{15}\text{N}$ values can be explained by a shift in red deer diet to
507 the edible parts of trees and shrubs available in inhabited forested areas.

508 Although biome analyses showed that the main habitats of red deer during the last 54 ka
509 years were different types of forests (coniferous, mixed and deciduous) (Niedziałkowska *et al.*,
510 2021), the results of isotopic values (i.e. $\delta^{13}\text{C}$ values above the -22.5‰) of most analysed samples
511 within the present study indicated that red deer often fed in more open habitats. The discrepancies
512 are probably caused by the different resolution of isotopic and biome analyses and the fact that the
513 “canopy effect” may be reflected through a threshold effect on the $\delta^{13}\text{C}$ values of collagen. Isotopic
514 analyses provide data on foraging habitats at the level of individuals, whereas biomes provide less

515 detailed information about habitats of occurrence on a larger spatial scale. Moreover, as revealed by
516 studies on modern red deer from the Białowieża Primeval Forest (Poland), even red deer inhabiting
517 forested areas preferred foraging in forest gaps than in closed forest (Kuijper *et al.*, 2009).

518 The variability of $\delta^{13}\text{C}$ values in red deer dated to the Holocene is best explained by the
519 percentage of forest cover (negative association) and mean July temperature (positive association).
520 Plants growing under a closed canopy, in poorly ventilated, more humid and shaded conditions,
521 showed depletion of ^{13}C abundance compared to those from open habitats (Tieszen, 1991; Bonafini
522 *et al.*, 2013). These results are consistent with analyses conducted on modern red deer (Sykut *et al.*,
523 2021) and other ungulates (Hofman-Kamińska *et al.*, 2018) indicating that the percentage of forest
524 cover is the most important factor explaining variability of $\delta^{13}\text{C}$ in bone collagen. The modeling
525 included samples dated to last 10 ka, therefore different factors caused by natural processes and
526 human activity had impact on the obtained results.

527 Considering the positive association between $\delta^{13}\text{C}$ values and mean July temperature, it
528 must be acknowledged that there is no clear explanation for such relationship (Heaton, 1999).
529 However, our results correspond with the findings of Van Klinken *et al.* (1994) who observed a
530 positive correlation between July temperature and bone $\delta^{13}\text{C}$ values during the Holocene. In our
531 study the Holocene red deer records with the highest July temperature were located in southern
532 Europe, where forest cover was also lower than in more northern areas of the continent at this time
533 (this study Tab. S4, comp. Fyfe *et al.*, 2015; Woodbridge *et al.*, 2018) due to climatic conditions
534 and human impact. Red deer inhabiting these areas probably forage in more open habitats, and
535 therefore they exhibited higher $\delta^{13}\text{C}$ values than individuals from other regions of Europe. Another
536 explanation of high $\delta^{13}\text{C}$ values of red deer from southern Europe could be the abundance of C4
537 plants in this part of Europe (Pyankov *et al.* 2010). In European temperate and boreal ecosystems,
538 woody and herbaceous C3 plants represent significantly higher $\delta^{13}\text{C}$ values than C4 plants (Dawson
539 *et al.* 2002).

540 Among analyzed climatic and environmental factors, variability of $\delta^{15}\text{N}$ is best explained by
541 mean July temperature (positive association), annual precipitation (negative association) and
542 altitude (negative association). Temperature and aridity changes are climatic parameters driving
543 significant oscillations in soil activity in modern as well as in ancient ecosystems and in
544 consequence cause shift of $\delta^{15}\text{N}$ values in plants further foraged by herbivores (Drucker *et al.*, 2011
545 and references therein). A similar relationship with mean annual temperature was observed in
546 studies on modern European bison (Hofman-Kamińska *et al.*, 2018). Additionally, higher $\delta^{15}\text{N}$
547 values are present in graminoids (grasses and sedges), and forbs than in shrubs and trees
548 (Nadelhoffer *et al.*, 1996; Ben-David *et al.*, 2001). Such types of plants more often grow in open
549 areas, such as grasslands, meadows and pastures, which explains why the percentage of open area is
550 the most important factor determining variability of $\delta^{15}\text{N}$ in modern populations of European red
551 deer (Sykut *et al.*, 2021).

552 In agreement with the results of present study, the altitude has been also proven to influence
553 the $\delta^{15}\text{N}$ values of modern herbivores. Such relationships was observed in hair of ungulates pastured
554 at the altitude ranging from 400 to 2500 m.a.s.l., the $\delta^{15}\text{N}$ values decreased c. 1.1‰ per 1000 m
555 (Männel *et al.*, 2007). Although we analysed locations from -103 to 1646 m.a.s.l., we obtained
556 similar results. The decreasing trend in $\delta^{15}\text{N}$ values are attributed to the lower mineralisation rate
557 and net nitrification rate at higher altitude (Sah & Brumme, 2003). However, the highest impact of
558 altitude on the $\delta^{15}\text{N}$ values can be expected in localities at high altitudes, above around 3200 m.a.s.l.
559 (Zech *et al.*, 2011). Similar relationship was observed in the Holocene in Western Alps, where the
560 decrease of $\delta^{15}\text{N}$ values in red deer bone collagen was related to the upward migration of the
561 individuals (Drucker *et al.*, 2011).

562 The overlapping values of stable isotopic composition of European red deer and wapiti dated
563 to the Late Pleistocene and the Holocene indicated in this study, may suggest that the foraging
564 habitats of these two species were more similar in the past than in the modern times but further
565 studies (including more wapiti samples) are needed to confirm this hypothesis. Additionally, we

566 found no association between the isotopic composition and haplogroups of red deer (Fig. S3).
567 However, the wide range of $\delta^{13}\text{C}$ and $\delta^{15}\text{N}$ values in red deer bones and the variability of biomes,
568 where they have occurred during the last 50 ka years (comp. Niedziałkowska *et al.*, 2021), revealed
569 that they have had wide ecological niches and were able to adapt to different environmental
570 conditions. Further studies are needed to confirm similar flexibility in case of wapiti.

571 **5. Conclusions**

During the Late Pleistocene and Holocene (last 50 ka) in Europe and Asia, red deer shifted their feeding habitats according to environmental changes (e.g. forest expansion related to climate warming), and also in response to landscape changes associated with human activity (i.e. deforestation and the spread of agriculture). Additionally, red deer feeding habitats analysed at the Eurasian scale differed regionally. According to isotopic analyses, contemporary red deer feed in the most densely forested areas in comparison with individuals over the past 50 ka. Surprisingly, the values of carbon and nitrogen stable isotopes of European red deer and wapiti overlapped. Among all analysed variables the variance of $\delta^{13}\text{C}$ in European red deer during the Holocene is best explained by forest cover and mean July temperature, while the variance of $\delta^{15}\text{N}$ is best explained by mean July temperature, annual precipitation and altitude. It's probably not altitude per se that is responsible for variance in $\delta^{15}\text{N}$, but soil types. Mountainous landscapes tend to have thin, nitrogen poor soils (often due to low organic content in the absence of rapid soil formation or addition of organic material). The results of this study have broadened understanding of the ecology of one of the most important game species in Eurasia in the last 50 ka. Moreover, presented in this study data can be useful in revealing human diet and environmental conditions since the Last Pleistocene in Europe.

572 Table 1. Multiple regression model selection (based on the AICc criteria) to investigate the effect of different factors on carbon ($\delta^{13}\text{C}$) stable
573 isotope compositions in bone collagen of the Holocene red deer *Cervus elaphus* from Europe. The first two models representing the highest
574 parsimony (the lowest AICc scores) have been selected as the best models; df - number of estimated parameters; AICc - Akaike's information
575 criterion with a second order correction for small sample sizes; ΔAICc - difference in AICc between a given model and the most parsimonious
576 model; ω_i - weight of the model.

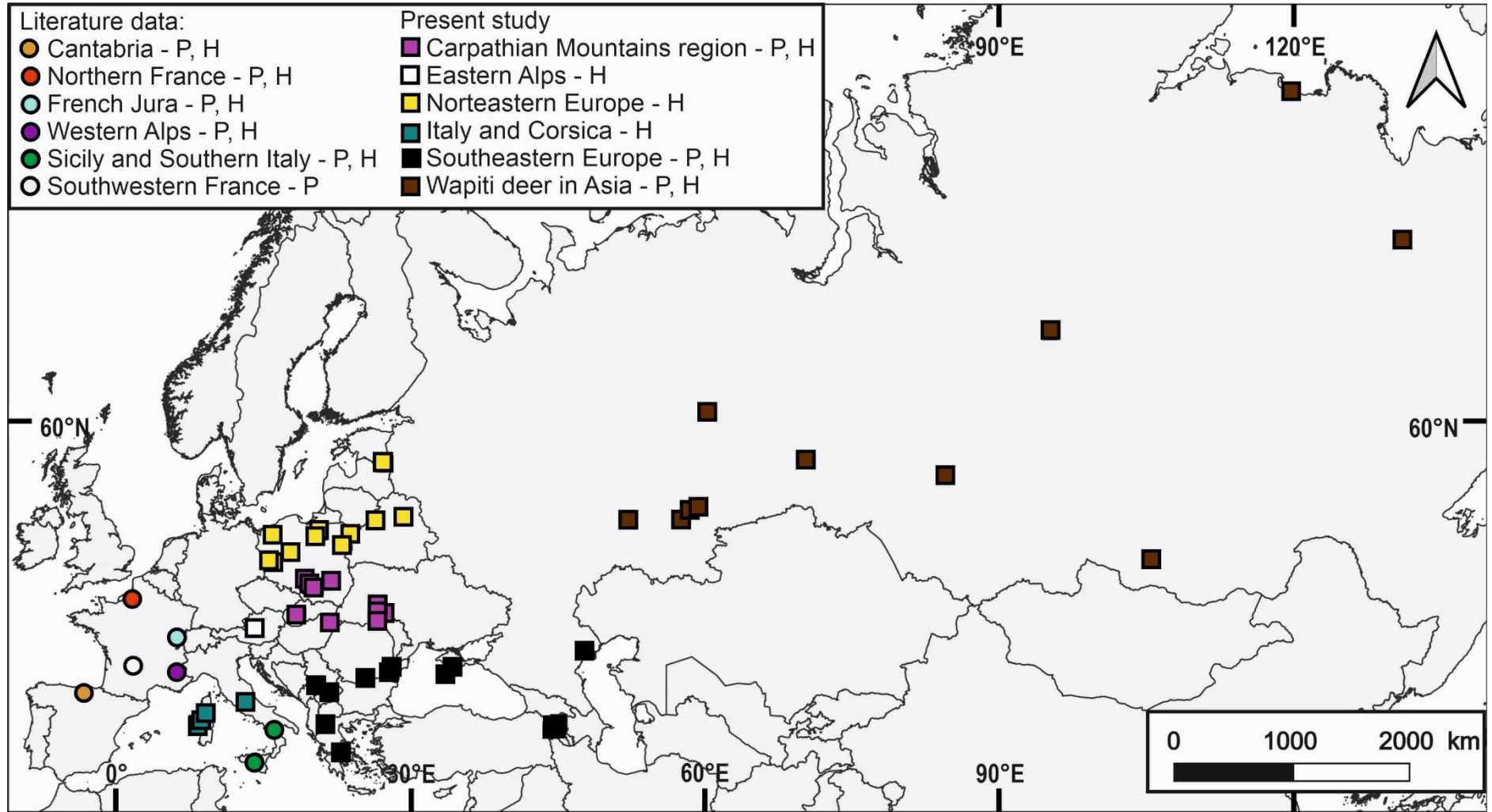
Variables	df	AICc	ΔAICc	ω_i
Median age + Forest	4	91.3	0	0.4568
Median age + July temperature	4	91.8	0.50	0.3559
Median age + MtDNA	5	95.5	4.14	0.0577
Median age + Annual precipitation	4	95.7	4.41	0.0505
Median age + July precipitation	4	95.1	3.80	0.0682
Intercept	2	100.6	9.26	0.0045
Median age + January mean temperature	4	101.3	9.95	0.0031
Median age + Biome	4	102.9	11.52	0.0014
Median age + January precipitation	4	104.1	12.72	0.0008
Median age + Annual precipitation	4	104.6	13.30	0.0006
Median age + Altitude	4	105.3	13.96	0.0004

577 Table 2. Multiple regression model selection (based on the AICc criteria) to investigate the effect of different factors on nitrogen ($\delta^{15}\text{N}$) stable
578 isotope compositions in bone collagen of Holocene red deer *Cervus elaphus* from Europe. Three models representing the highest parsimony (the
579 lowest AICc scores) have been selected as the best models; df -number of estimated parameters; AICc - Akaike's information criterion with a
580 second order correction for small sample sizes; ΔAICc - difference in AICc between a given model and the most parsimonious model; ω_i -
581 weight of the model.

Variables	df	AICc	ΔAICc	ω_i
Median age + July	4	129.0	0	0.2357
Median age + Annual	4	129.2	0.22	0.2108
Median age + Altitude	4	130.1	1.08	0.1373
Median age + July	4	130.8	1.79	0.0965
Median age + Annual	4	130.8	1.83	0.0943
Median age + MtDNA	5	131.7	2.72	0.0605
Median age + Forest	4	132.1	3.09	0.0503
Median age + January	4	132.4	3.38	0.0435
Median age + January	4	132.5	3.50	0.0409
Median age + Biome	4	133.1	4.14	0.0298
Intercept	2	141.5	12.49	0.0005

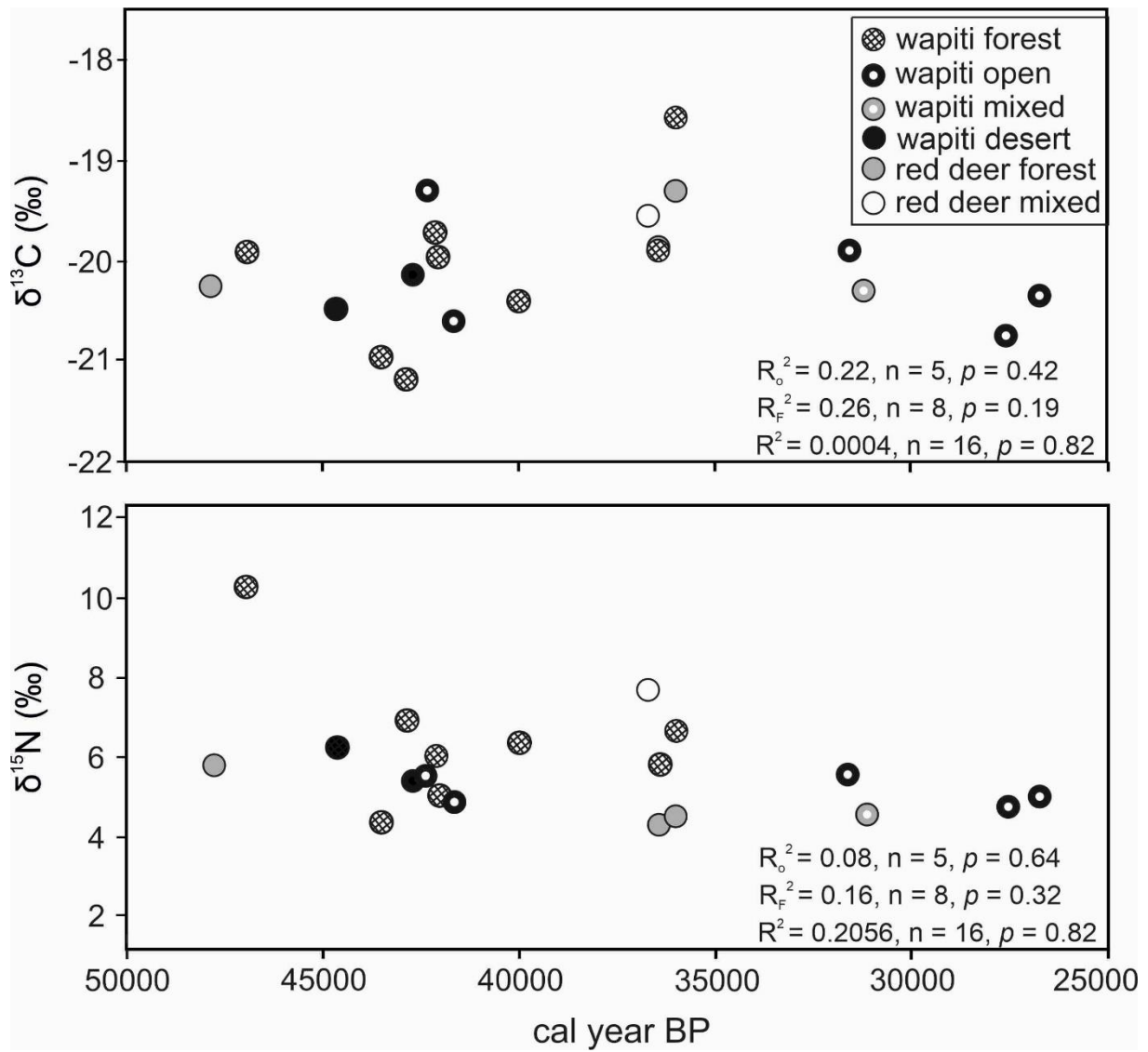
582

583



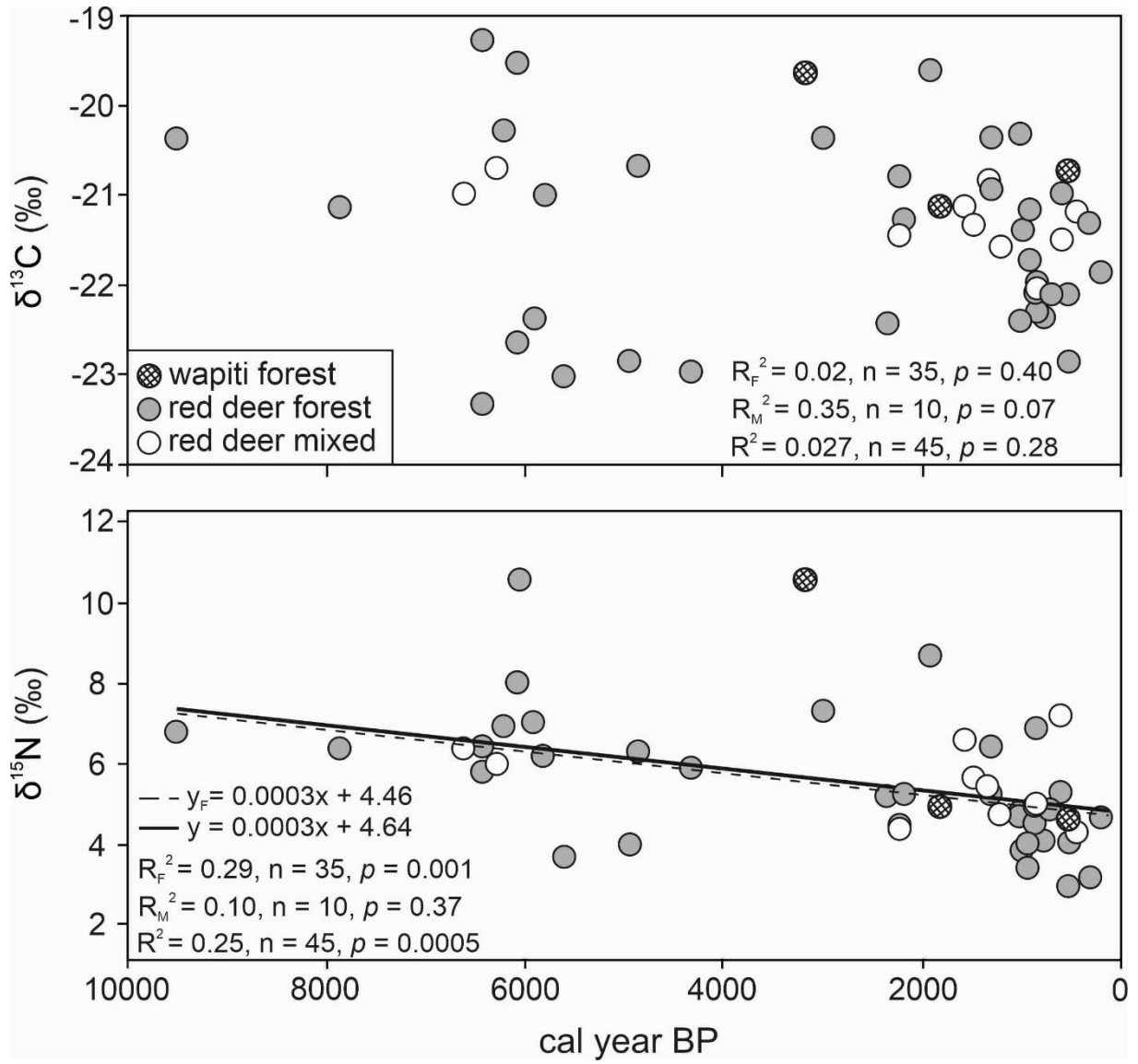
584

585 **Fig. 1**

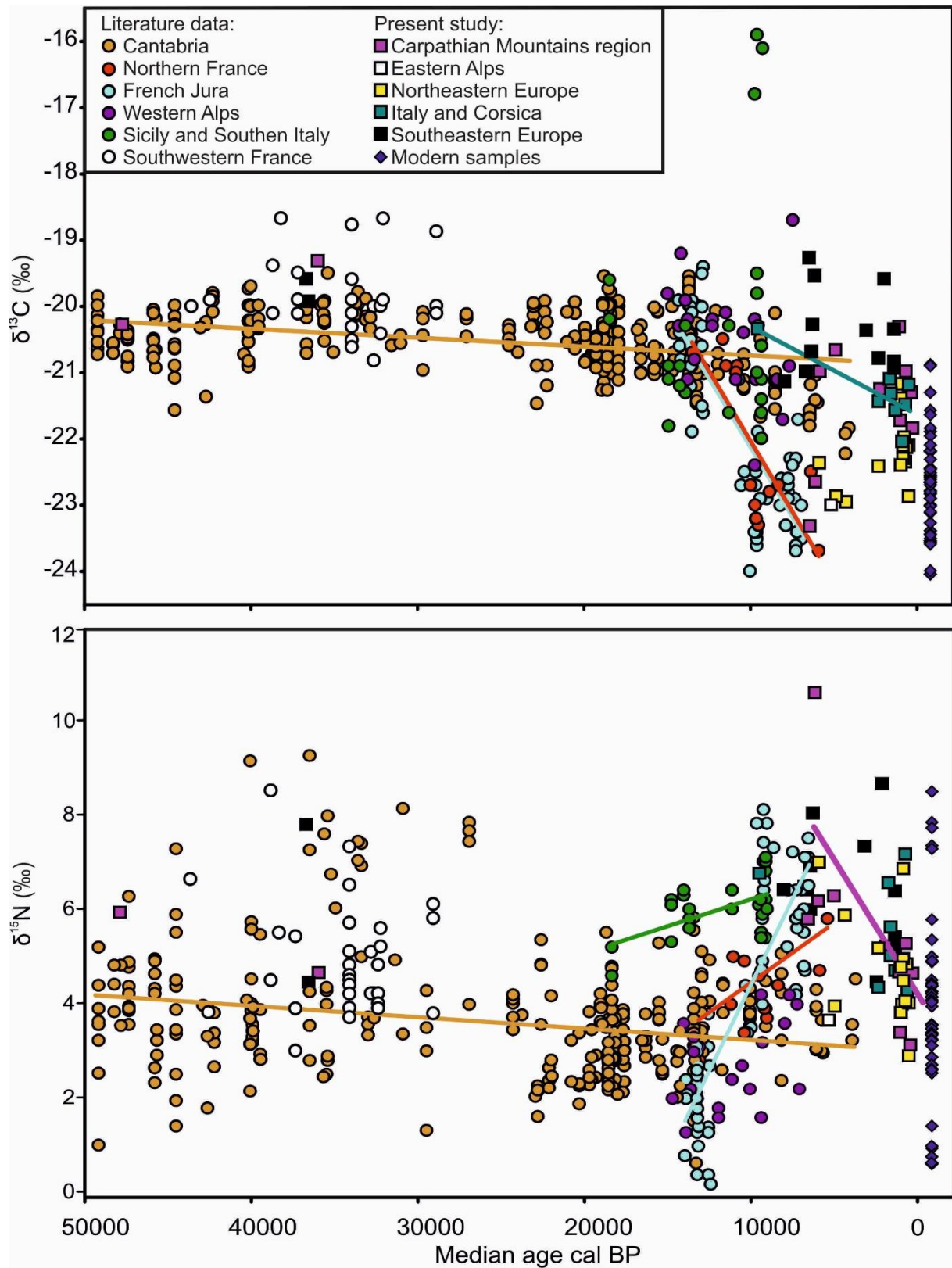


586

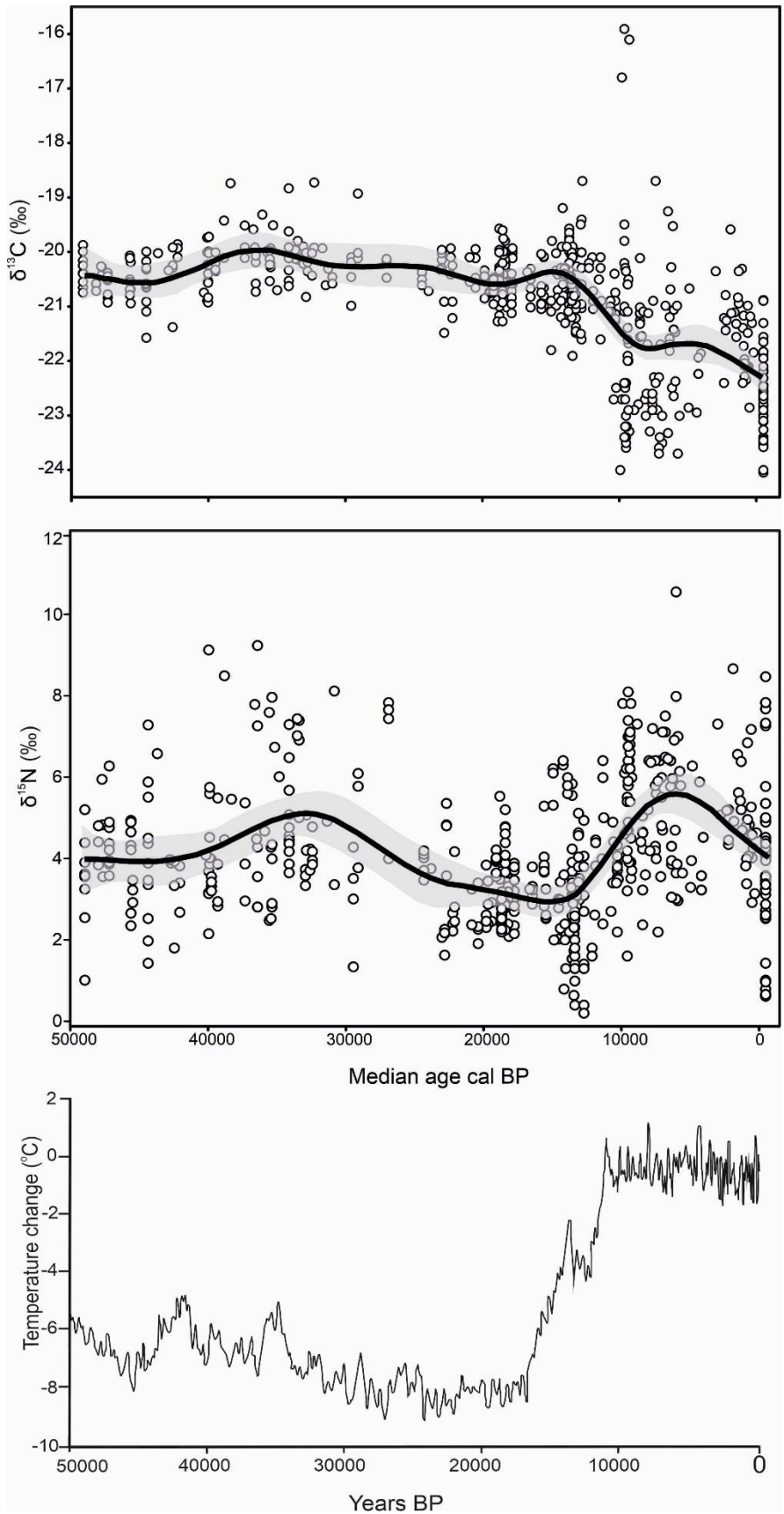
587 **Fig. 2**



590 **Fig. 3**

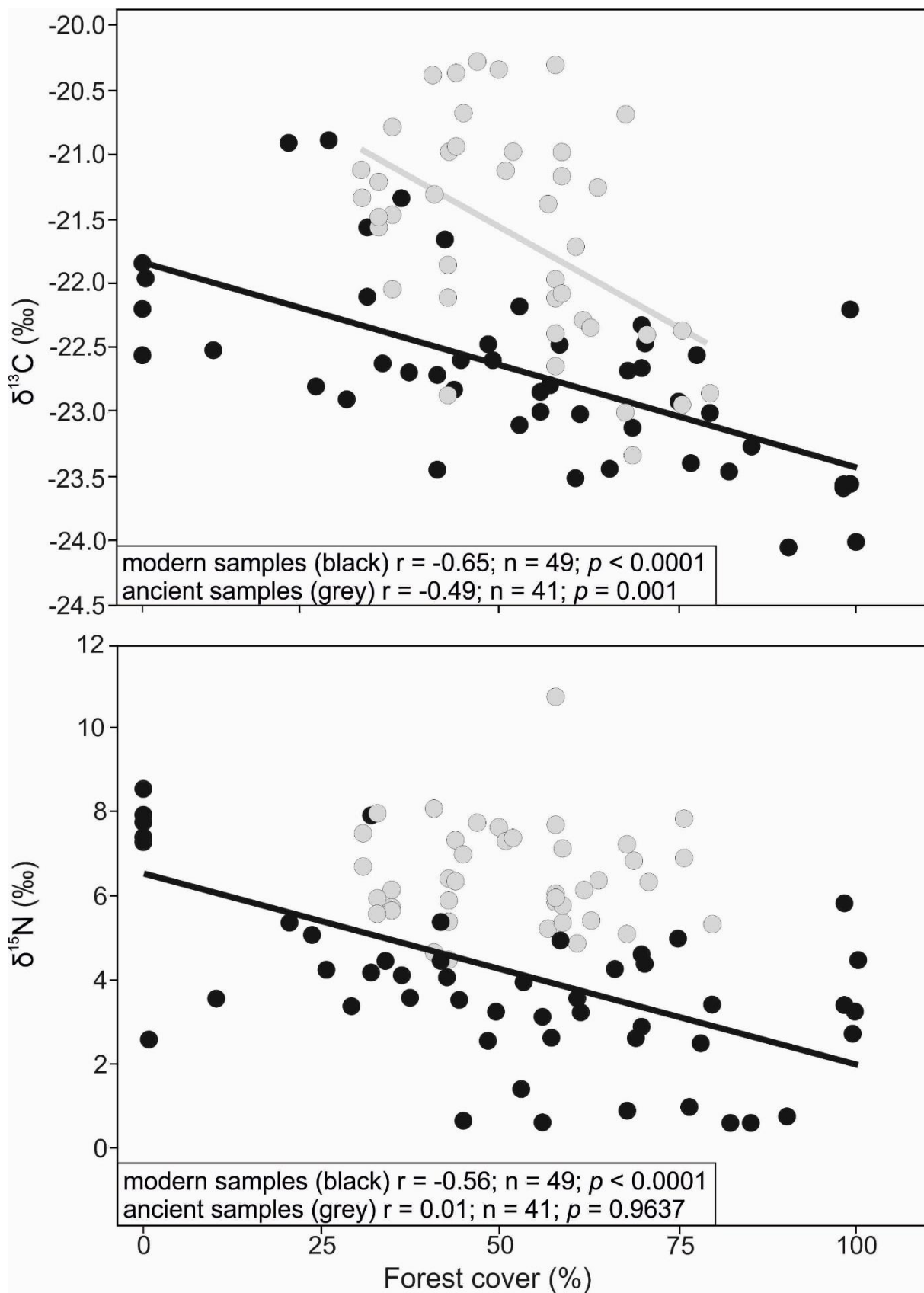


591
592 **Fig. 4**

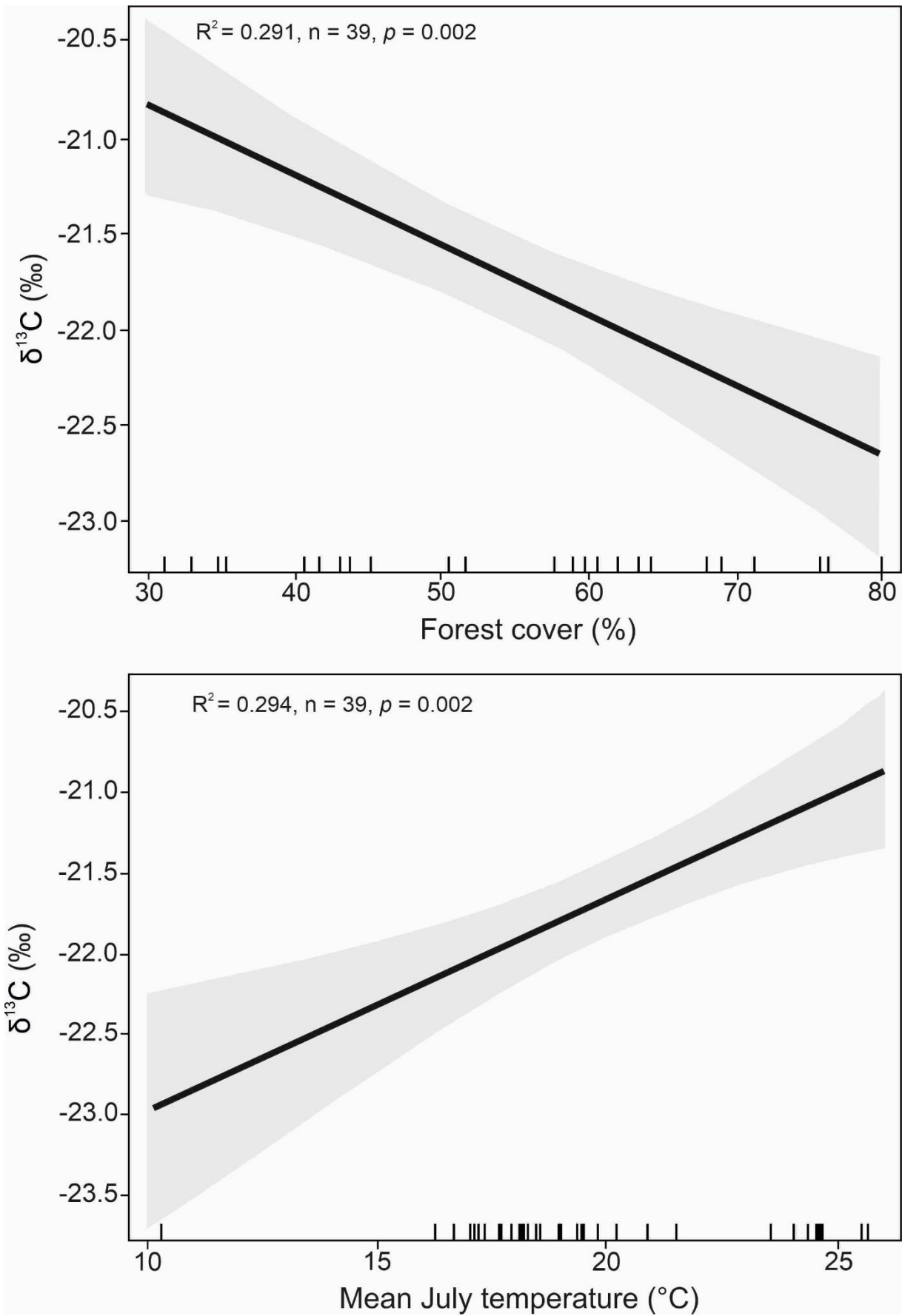


593

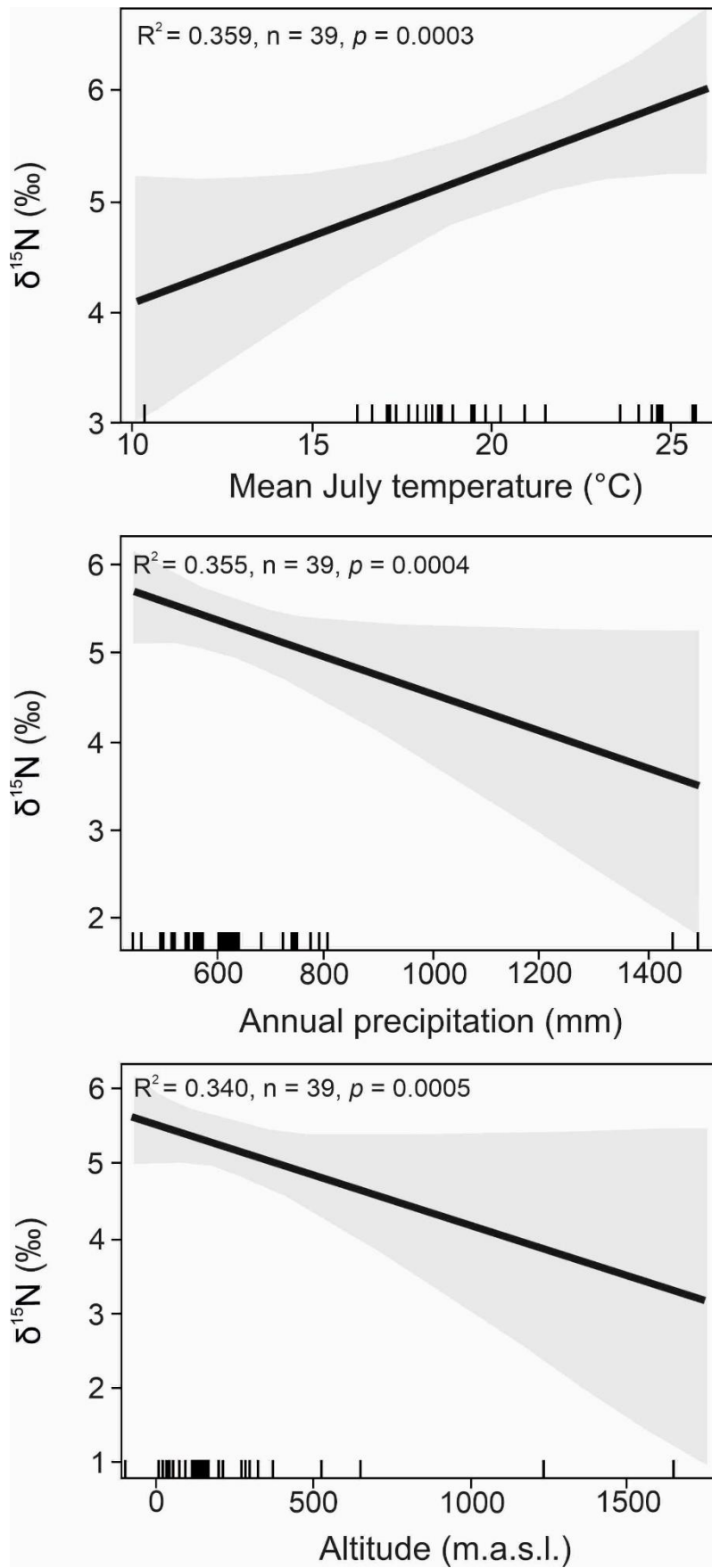
594 **Fig. 5**



597 **Fig. 6**



599
600 **Fig. 7**



601

602 **Fig. 8**

603 **Figures**

604 Fig. 1. Spatial distribution of the ancient European red deer and wapiti deer samples analysed
605 in the present study (Tab. S1) and location of sites where other studies (Tab. S2) on stable
606 isotopic analyses including radiocarbon-dated subfossil bones of *Cervus elaphus* were
607 performed. P – samples dated to the Late Pleistocene (50 000 - 26000 BP); H- samples dated
608 to the Holocene (11700 – 0 BP).

609 Fig. 2. Chronological changes in $\delta^{13}\text{C}$ (upper panel) and $\delta^{15}\text{N}$ (lower panel) of red deer (n = 4)
610 and wapiti (n = 16) during the Late Pleistocene. Wapiti biome categories: Forest - deciduous
611 taiga or montane forest; Open - shrub or steppe tundra; Mixed - xerophytic shrub or
612 sclerophyll woodland. The regression parameters were calculated for the wapiti samples only,
613 including all *C. canadensis* samples and separately for wapiti inhabiting forest (F) and open
614 (O) biomes. Wapiti from mixed and desert biomes were not included in the statistical
615 analyses. Red deer biome categories: Forest – deciduous montane or coniferous forest, Mixed
616 - sclerophyll woodland.

617 Fig. 3. Chronological changes in $\delta^{13}\text{C}$ (upper panel) and $\delta^{15}\text{N}$ (lower panel) and of red deer (n
618 = 45) and wapiti (n = 3) during the Holocene. Red deer biome categories: Forest – coniferous
619 or mixed forest; Mixed - xerophytic shrub or sclerophyll woodland. The regression
620 parameters were calculated for the European red deer samples only, including all *C. elaphus*
621 samples and separately for red deer inhabiting forest (F) and mixed (M) biomes. Wapiti
622 biome categories: Forest – coniferous or deciduous taiga.

623 Fig. 4. Chronological changes in $\delta^{13}\text{C}$ (upper panel) and $\delta^{15}\text{N}$ (lower panel) in *Cervus elaphus*
624 bones since the Late Pleistocene until the modern times in various localities in Europe. Data
625 from the ancient European red deer individuals from this study (n = 49, Tab S1), data from
626 the literature (n = 440, Tab. S2), and modern individuals (n = 49, Tab. S3, Sykut *et al.* 2021).

627 Fig. 5. Generalized Additive Model (GAM) plot showing changes in $\delta^{13}\text{C}$ (upper panel) and
628 $\delta^{15}\text{N}$ (middle panel) through time since the Late Pleistocene until modern times (the literature
629 data $n = 440$, this study $n = 55$, modern samples $n = 49$, for source of data see Tables S1–S3).
630 Lower panel: Antarctic (data from the Vostok ice core) temperature oscillations in the study
631 period (source: FAMOUS database; Smith & Gregory, 2012).

632 Fig. 6. Relationship between forest cover and $\delta^{13}\text{C}$ (upper panel), and $\delta^{15}\text{N}$ (lower panel) for
633 ancient (9 508 – 189 cal BP, $n = 41$) and modern red deer ($n = 49$) samples.

634 Fig. 7. Relationship between carbon stable isotope composition ($\delta^{13}\text{C}$) in bone collagen of
635 ancient European red deer ($n = 39$) and forest cover (upper panel), mean July temperature
636 (lower panel) based on estimates from multiple regression models. Grey areas – 95%
637 confidence intervals of the regression lines.

638 Fig. 8. Relationship between nitrogen stable isotope composition ($\delta^{15}\text{N}$) in bone collagen of
639 ancient European red deer samples ($n = 39$) and mean July temperature (upper panel), annual
640 precipitation (middle panel) and altitude (lower panel) based on estimates from multiple
641 regression models. Grey areas – 95% confidence intervals of the regression lines.

642 **Acknowledgments**

643 The study was financed by the National Science Centre, Poland (grant nos.
644 2016/23/N/NZ8/03995 and DEC-2013/11/B/NZ8/00888) and the budget of the Mammal
645 Research Institute Polish Academy of Sciences in Białowieża. The research was supported by
646 the Ministry of Science and Education through a special grant for the ^{14}C and Mass
647 Spectrometry Laboratory (209848/E-367/SPUB/2018/1). We thank John Stewart for the
648 Faunal Database of the Stage Three Project. The vegetation reconstruction of (Fyfe *et al.*,
649 2015) resulted from a project funded by the Leverhulme Trust (F00568W), which made use
650 of fossil pollen datasets from the European Pollen Database (EPD)
651 (<http://www.europeanpollendatabase.net/>); the work of the data contributors and the EPD
652 community is gratefully acknowledged. Data from FAMOUS climate model simulations were
653 provided by Robin S. Smith through the National Centre for Atmospheric Science and the
654 Centre for Environmental Data Analysis, UK. We thank A. Wiszniowska for the help with
655 laboratory analyses and B. Jędrzejewska for comments on this manuscript. We are grateful for
656 the Museum of the Institute of Plant and Animal Ecology (UB RAS, Ekaterinburg) for
657 providing specimens.

658

659 **Conflict of interest**

660 The authors declare no conflict of interest

661 **References**

- 662 Alekseeva, E.V. (1980) *Mlekopitajuszczyje plejstocena yugo-vostoka Zapadnoj Sibiri*
663 *(hiszczynije, hobotnyje, kopytnyje)* (pp. 188). Moskva: Izdatelstvo Nauka [In Russian].
- 664 Ambrose, S.H. (1990) Preparation and characterization of bone and tooth collagen for
665 isotopic analysis. *Journal of Archaeological Science*, **17**, 431-451.
- 666 Ambrose S.H., Norr L. (1993) Experimental Evidence for the Relationship of the Carbon
667 Isotope Ratios of Whole Diet and Dietary Protein to Those of Bone Collagen and
668 Carbonate. In J.B. Lambert, & G Grupe (Eds.), *Prehistoric Human Bone* (pp. 1-37).
669 Berlin, Heidelberg: Springer.
- 670 Amundson, R., Austin, A. T., Schuur, E. A. G., Yoo, K., Matzek, V., Kendall, C., Uebersax,
671 A., Brenner, D., and Baisden, W. T. (2003), Global patterns of the isotopic
672 composition of soil and plant nitrogen, *Global Biogeochem. Cycles*, **17**, 1031.
- 673 Anderson, D.E., Goudie, A.S. & Parker, A.G. (2007) Environmental Change in Post-glacial
674 Times. *Global Environments through the Quaternary* (pp. 154-196). Oxford: Oxford
675 University Press.
- 676 Apollonio, M., Anderson, R. & Putman, R. (2010) *European Ungulates and Their*
677 *Management in the 21st Century*. Cambridge, UK: Cambridge University Press.
- 678 Bartoń, K. (2013) *MuMIn: Multi-model inference*. R package version 1.9. 13. The
679 Comprehensive R Archive Network (CRAN): Vienna, Austria.
- 680 Ben-David, M., Shochat, E. & Adams, L.G. (2001) Utility of stable isotope analysis in
681 studying foraging ecology of herbivores: Examples from moose and caribou. *Alces*,
682 **37**, 421-434.
- 683 Bocherens, H., Drucker, D.G. & Madelaine, S. (2014) Evidence for a ¹⁵N positive excursion
684 in terrestrial foodwebs at the Middle to Upper Palaeolithic transition in south-western
685 France: Implications for early modern human palaeodiet and palaeoenvironment.
686 *Journal of Human Evolution*, **69**, 31-43.
- 687 Bocherens, H., Hofman-Kamińska, E., Drucker, D.G., Schmölcke, U. & Kowalczyk, R.
688 (2015) European bison as a refugee species? Evidence from Isotopic Data on Early
689 Holocene Bison and Other Large Herbivores in Northern Europe. *PLOS ONE*, **10**,
690 e0115090.
- 691 Bonafini, M., Pellegrini, M., Ditchfield, P. & Pollard, A.M. (2013) Investigation of the
692 ‘canopy effect’ in the isotope ecology of temperate woodlands. *Journal of*
693 *Archaeological Science*, **40**, 3926-3935.
- 694 Borowik, T., Cornulier, T. & Jędrzejewska, B. (2013) Environmental factors shaping ungulate
695 abundances in Poland. *Acta Theriologica*, **58**, 403-413.
- 696 Brand, W. & Coplen, T. (2012) Stable isotope deltas: Tiny, yet robust signatures in nature.
697 *Isotopes in Environmental and Health Studies*, **48**, 393-409.
- 698 Bronk Ramsey, C. (2009) Bayesian Analysis of Radiocarbon Dates. *Radiocarbon*, **51**, 337-
699 360.
- 700 Brook, S., Pluháček, J., Lorenzini, R., Lovari, S., Masseti, M., Pereladova, O. & Mattioli, S.
701 (2018) *Cervus canadensis* (errata version published in 2019). *The IUCN Red List of*
702 *Threatened Species 2018*.
- 703 Burnham, K.P. & Anderson, D.R. (2002) *Model selection and multi-model inference: a*
704 *practical information-theoretic approach*. New York, NY: Springer.
- 705 Cerling, T.E., Harris, J.M., MacFadden, B.J., Leakey, M.G., Quade, J., Eisenmann, V. &
706 Ehleringer, J.R. (1997) Global vegetation change through the Miocene/Pliocene
707 boundary. *Nature*, **389**, 153-158.
- 708 Castaños, J., Zuluaga, MC., Ortega, LÁ., Murelaga, X., Alonso-Olazabal, A., Rofes, J.,
709 Castaños, J. (2014) Carbon and nitrogen stable isotopes of bone collagen of large

- 710 herbivores from the Late Pleistocene Kiputz IX cave site (Gipuzkoa, north Iberian
711 Peninsula) for palaeoenvironmental reconstruction. *Quaternary International*. **339–**
712 **340**, 131–138.
- 713 Chen, H., Ma, J., Li, F., Sun, Z., Wang, H., Luo, L. & Li, F. (1998) Seasonal composition and
714 quality of red deer *Cervus elaphus* diets in northeastern China. *Acta Theriologica*, **43**,
715 77–94.
- 716 Clark, P.U., Dyke, A.S., Shakun, J.D., Carlson, A.E., Clark, J., Wohlfarth, B., Mitrovica, J.X.,
717 Hostetler, S.W. & McCabe, A.M. (2009) The last glacial maximum. *Science*, **325**,
718 710–714.
- 719 Clutton-Brock, T.H., Albon, S.D. (1989) *Red Deer in the Highlands*. Oxford, UK: BSP
720 Professional Books.
- 721 Coplen, T. B., Brand, W. A., Gehre, M., Gröning, M., Meijer, H. A., Toman, B., Verkouteren,
722 R. M., & International Atomic Energy Agency (2006). After two decades a second
723 anchor for the VPDB delta¹³C scale. *Rapid communications in mass spectrometry :
724 RCM*, **20**(21), 3165–3166.
- 725 Craig, O.E., Biazzo, M., Colonese, A.C., Di Giuseppe, Z., Martinez-Labarga, C., Lo Vetro,
726 D., Lelli, R., Martini, F., & Rickards, O. (2010). Stable isotope analysis of Late Upper
727 Palaeolithic human and faunal remains from Grotta del Romito (Cosenza), Italy.
728 *Journal of Archaeological Science*, **37**(10), 2504–2512.
- 729 Croitor, R. & Obada, T. (2018) On the presence of Late Pleistocene wapiti, *Cervus*
730 *canadensis* Erxleben, 1777 (Cervidae, Mammalia) in the Palaeolithic site Climăuți II
731 (Moldova). *Contributions to Zoology, Naturalis*, **87**, hal-01737219.
- 732 Davis, B.A.S., Brewer, S., Stevenson, A.C. & Guiot, J. (2003) The temperature of Europe
733 during the Holocene reconstructed from pollen data. *Quaternary Science Reviews*, **22**,
734 1701–1716.
- 735 Dawson, T.E., Mambelli, S., Plamboeck, A.H., Templer, P.H., & Tu, K.P. (2002). Stable
736 isotopes in plant ecology. *Annual review of ecology and systematics*, **33**(1), 507–559.
- 737 DeNiro, M.J. (1985) Postmortem preservation and alteration of in vivo bone collagen isotope
738 ratios in relation to palaeodietary reconstruction. *Nature*, **317**, 806–809.
- 739 Dixon, G., Marriott, A., Stelfox, G., Dunkerley, C. & Batke, S. (2021) How do red deer react
740 to increased visitor numbers? A case study on human-deer encounter probability and
741 its effect on cortisol stress responses. *Nature Conservation*, **43**, 55–78.
- 742 Di Maida, G., Mannino, M., Krause-Kyora, B., Jensen, T., Talamo, S. (2019) Radiocarbon
743 dating and isotope analysis on the purported Aurignacian skeletal remains from
744 Fontana Nuova (Ragusa, Italy). *PLOS ONE*, **14**, e0213173.
- 745 Doan, K., Zachos FE., Wilkens, B., Vigne JD., Piotrowska, N., Stanković A., Jędrzejewska,
746 B., Stefaniak, K. & Niedziałkowska, M. (2017) Phylogeography of the Tyrrhenian red
747 deer (*Cervus elaphus corsicanus*) resolved using ancient DNA of radiocarbon-dated
748 subfossils. *Scientific Reports*, **7**, 2331.
- 749 Doan, K., Niedziałkowska, M., Stefaniak, K., Sykut, M., Jędrzejewska, B., Ratajczak-
750 Skrzatek, U., Piotrowska, N., Ridush, B., Zachos, F.E., Popović, D., Baca, M.,
751 Mackiewicz, P., Kosintsev, P., Makowiecki, D., Charniauski, M., Boeskorov, G.,
752 Bondarev, A.A., Danila, G., Kusak, J., Rannamäe, E., Saarma, U., Arakelyan, M.,
753 Manaseryan, N., Krasnodębski, D., Titov, V., Hulva, P., Bălășescu, A., Trantalidou,
754 K., Dimitrijević, V., Shpansky, A., Kovalchuk, O., Klementiev, A.M., Foronova, I.,
755 Malikov, D.G., Juras, A., Nikolskiy, P., Grigoriev, S.E., Cheprasov, M.Y.,
756 Novgorodov, G.P., Sorokin, A.D., Wilczyński, J., Protopopov, A.V., Lipecki, G. &
757 Stanković, A. (2022) Phylogenetics and phylogeography of red deer mtDNA lineages
758 during the last 50 000 years in Eurasia. *Zoological Journal of the Linnean Society* **194**,
759 431–456.

- 760 Drucker, D.G., Bocherens, H., Bridault, A. & Billiou, D. (2003a) Carbon and nitrogen
761 isotopic composition of red deer (*Cervus elaphus*) collagen as a tool for tracking
762 palaeoenvironmental change during the Late-Glacial and Early Holocene in the
763 northern Jura (France). *Palaeogeography, Palaeoclimatology, Palaeoecology*, **195**,
764 375-388.
- 765 Drucker, D.G., Bocherens, H. & Billiou, D. (2003b) Evidence for shifting environmental
766 conditions in Southwestern France from 33 000 to 15 000 years ago derived from
767 carbon-13 and nitrogen-15 natural abundances in collagen of large herbivores. *Earth
768 and Planetary Science Letters*, **216**, 163-173.
- 769 Drucker, D.G., Bridault, A., Hobson, K.A., Szuma, E. & Bocherens, H. (2008) Can carbon-13
770 in large herbivores reflect the canopy effect in temperate and boreal ecosystems?
771 Evidence from modern and ancient ungulates. *Palaeogeography, Palaeoclimatology,
772 Palaeoecology*, **266**, 69-82.
- 773 Drucker, D.G. & Bocherens, H. (2009) Carbon stable isotopes of mammal bones as tracers of
774 canopy development and habitat use in temperate and boreal contexts. In J.D.
775 Creighton & P.J. Roney (Eds.), *Forest Canopies: Forest Production, Ecosystem
776 Health, and Climate Conditions* (pp. 103-109). New York, NY: Nova Science
777 Publishers.
- 778 Drucker, D.G., Hobson, K., Ouellet, J.-P. & Courtois, R. (2010) Influence of forage
779 preferences and habitat use on ¹³C and ¹⁵N abundance in wild caribou (*Rangifer
780 tarandus caribou*) and moose (*Alces alces*) from Canada. *Isotopes in Environmental
781 and Health Studies*, **46**, 107-21.
- 782 Drucker, D.G., Bridault, A., Cupillard, C., Hujic, A. & Bocherens, H. (2011) Evolution of
783 habitat and environment of red deer (*Cervus elaphus*) during the Late-glacial and early
784 Holocene in eastern France (French Jura and the western Alps) using multi-isotope
785 analysis ($\delta^{13}\text{C}$, $\delta^{15}\text{N}$, $\delta^{18}\text{O}$, $\delta^{34}\text{S}$) of archaeological remains. *Quaternary International*,
786 **245**, 268-278.
- 787 Drucker, D.G., Bridault, A., Ducrocq, T., Bauman, C., Valentin, F. (2020) Environment and
788 human subsistence in Northern France at the Late Glacial to early Holocene transition.
789 *Archaeological and Anthropological Sciences*, **12**, 194.
- 790 ESRI (2015) ArcGIS Desktop: Release 10.1. Environmental Systems Research Institute:
791 Redlands, CA.
- 792 Feng, X. (1998) Long-term ci/ca response of trees in western North America to atmospheric
793 CO₂ concentration derived from carbon isotope chronologies. *Oecologia*, **117**, 19-25.
- 794 Foronova, I. (1999) Quaternary mammals and stratigraphy of the Kuznetsk Basin (South-
795 western Siberia). *Sbornik Geologických Ved-Antropozoikum*, **23**, 71-97.
- 796 Foronova, I. (2001) Quaternary mammals of the South-East of Western Siberia (Kuznetsk
797 Basin): phylogeny, biostratigraphy, and palaeoecology. Novosibirsk: Publishing
798 House of Siberian Branch, Russian Academy of Sciences, GEO.
- 799 Fox, J. & Weisberg, S. (2019) *An R Companion to Applied Regression*, (3rd ed). Thousand
800 Oaks, CA: Sage.
- 801 Fyfe, R.M., Woodbridge, J. & Roberts, N. (2015) From forest to farmland: pollen-inferred
802 land cover change across Europe using the pseudobiomization approach. *Global
803 Change Biology*, **21**, 1197-1212.
- 804 Gebert, C. & Verheyden-Tixier, H. (2001) Variations of diet composition of Red deer (*Cervus
805 elaphus* L.) in Europe. *Mammal Review*, **31**, 189-201.
- 806 Geist, V. (1998) *Deer of the World: Their Evolution, Behaviour, and Ecology*.
807 Mechanicsburg: Stackpole Books.

- 808 Gignoux, C.R., Henn, B.M. & Mountain, J.L. (2011) Rapid, global demographic expansions
809 after the origins of agriculture. *Proceedings of the National Academy of Sciences*, **108**,
810 6044-6049.
- 811 Giroux, M.-A., Valiquette, É., Tremblay, J.-P. & Côté, S.D. (2015) Isotopic Differences
812 between Forage Consumed by a Large Herbivore in Open, Closed, and Coastal
813 Habitats: New Evidence from a Boreal Study System. *PLOS ONE*, **10**, e0142781.
- 814 Gonfiantini, R., Rozanski, K. & Stichler, W. (1990) Intercalibration of Environmental Isotope
815 Measurements: The Program of the International Atomic Energy Agency.
816 *Radiocarbon*, **32**, 369-374.
- 817 Heaton, T.H.E. (1999) Spatial, Species, and Temporal Variations in the ¹³C/¹²C Ratios of
818 C3Plants: Implications for Palaeodiet Studies. *Journal of Archaeological Science*, **26**,
819 637-649.
- 820 Hofman-Kamińska, E., Bocherens, H., Borowik, T., Drucker, D.G. & Kowalczyk, R. (2018)
821 Stable isotope signatures of large herbivore foraging habitats across Europe. *PLOS*
822 *ONE*, **13**, e0190723.
- 823 Hofman-Kamińska, E., Bocherens, H., Drucker, D.G., Fyfe, R.M., Gumiński, W.,
824 Makowiecki, D., Pacher, M., Piličiauskienė, G., Samojlik, T., Woodbridge, J. &
825 Kowalczyk, R. (2019) Adapt or die - response of large herbivores to environmental
826 changes in Europe during the Holocene. *Global Change Biology*, **25**, 2915-2930.
- 827 Iacumin, P., Nikolaev, V. & Ramigni, M. (2000) C and N stable isotope measurements on
828 Eurasian fossil mammals, 40 000 to 10 000 years BP: Herbivore physiologies and
829 palaeoenvironmental reconstruction. *Palaeogeography, Palaeoclimatology,*
830 *Palaeoecology*, **163**, 33-47.
- 831 Jones, J. R., Richards, M. P., Straus, L. G., Reade, H., Altuna, J., Mariezkurrena, K., &
832 Marín-Arroyo, A. B. (2018). Changing environments during the Middle-Upper
833 Palaeolithic transition in the eastern Cantabrian Region (Spain): direct evidence from
834 stable isotope studies on ungulate bones. *Scientific reports*, **8**(1), 14842.
- 835 Jones, J. R., Richards, M. P., Reade, H., de Quirós, F. B., & Marín-Arroyo, A. B. (2019).
836 Multi-Isotope investigations of ungulate bones and teeth from El Castillo and
837 Covalejos caves (Cantabria, Spain): Implications for paleoenvironment
838 reconstructions across the Middle-Upper Palaeolithic transition. *Journal of*
839 *Archaeological Science: Reports*, **23**, 1029-1042.
- 840 Jones, J. R., Marín-Arroyo, A. B., Straus, L. G., & Richards, M. P. (2020). Adaptability,
841 resilience and environmental buffering in European Refugia during the Late
842 Pleistocene: Insights from La Riera cave (Asturias, cantabria, Spain). *Scientific*
843 *reports*, **10**(1), 1-17.
- 844 Kerley, G. I., Kowalczyk, R., & Cromsigt, J. P. (2012) Conservation implications of the
845 refugee species concept and the European bison: king of the forest or refugee in a
846 marginal habitat?. *Ecography*, **35**(6), 519-529.
- 847 Kuijper, D.P.J., Cromsigt, J.P.G.M., Churski, M., Adam, B., Jędrzejewska, B. &
848 Jędrzejewski, W. (2009) Do ungulates preferentially feed in forest gaps in European
849 temperate forest? *Forest Ecology and Management*, **258**, 1528-1535.
- 850 Kuznetsova, A., Brockhoff, P.B., Christensen, R.H.B. (2017) “lmerTest Package: Tests in
851 Linear Mixed Effects Models.” *Journal of Statistical Software*, **82**, 1–26.
- 852 Liu, X.-Z., Zhang, Y., Li, Z.-G., Feng, T., Su, Q. & Song, Y. (2017) Carbon isotopes of C3
853 herbs correlate with temperature on removing the influence of precipitation across a
854 temperature transect in the agro-pastoral ecotone of northern China. *Ecology and*
855 *Evolution*, **7**, 10582-10591.

- 856 Lone, K., Loe, L.E., Meisingset, E.L., Stamnes, I. & Mysterud, A. (2015) An adaptive
857 behavioural response to hunting: surviving male red deer shift habitat at the onset of
858 the hunting season. *Animal Behaviour*, **102**, 127-138.
- 859 Longin, R. (1971) New Method of Collagen Extraction for Radiocarbon Dating. *Nature*, **230**,
860 241-242.
- 861 Lorenzini, R. & Garofalo, L. (2015) Insights into the evolutionary history of *Cervus*
862 (*Cervidae*, tribe *Cervini*) based on Bayesian analysis of mitochondrial marker
863 sequences, with first indications for a new species. *Journal of Zoological Systematics*
864 *and Evolutionary Research*, **53**, 340-349.
- 865 Lovari, S., Lorenzini, R., Masseti, M., Pereladova, O., Carden, R., Brook, S. & Mattioli, S.
866 (2018) *Cervus elaphus* (amended version of 2016 assessment). *The IUCN Red List of*
867 *Threatened Species 2018*.
- 868 Ludt, C.J., Schroeder, W., Rottmann, O. & Kuehn, R. (2004) Mitochondrial DNA
869 phylogeography of red deer (*Cervus elaphus*). *Molecular Phylogenetics and*
870 *Evolution*, **31**, 1064-1083.
- 871 Männel, T.T., Auerswald, K. & Schnyder, H. (2007) Altitudinal gradients of grassland carbon
872 and nitrogen isotope composition are recorded in the hair of grazers. *Global Ecology*
873 *and Biogeography*, **16**, 583-592.
- 874 Mannino, M. A., Di Salvo, R., Schimmenti, V., Di Patti, C., Incarbona, A., Sineo, L., &
875 Richards, M. P. (2011a). Upper Palaeolithic hunter-gatherer subsistence in
876 Mediterranean coastal environments: an isotopic study of the diets of the earliest
877 directly-dated humans from Sicily. *Journal of Archaeological Science*, **38**(11), 3094–
878 3100.
- 879 Mannino, M. A., Thomas, K. D., Leng, M. J., Di Salvo, R., & Richards, M. P. (2011b). Stuck
880 to the shore? Investigating prehistoric hunter-gatherer subsistence, mobility and
881 territoriality in a Mediterranean coastal landscape through isotope analyses on marine
882 mollusc shell carbonates and human bone collagen. *Quaternary International*, **244**(1),
883 88–104.
- 884 Markova, A., van Kolfschoten, T., Bohnke, S. J. P., Kosinsev, P. A., Mol, J., Puzachenko, A.,
885 Simakova, A. N., Smirnov, N. G., Verpoorte, A. & Golovachev, I. B. (2008) *Evolution*
886 *of European Ecosystems during Pleistocene–Holocene Transition (24–8 Kyr BP)*.
887 Moscow: KMK Scientific Press.
- 888 Marquer, L., Gaillard, M.-J., Sugita, S., Poska, A., Trondman, A.-K., Mazier, F., Nielsen,
889 A.B., Fyfe, R.M., Jönsson, A.M. & Smith, B. (2017) Quantifying the effects of land
890 use and climate on Holocene vegetation in Europe. *Quaternary Science Reviews*, **171**,
891 20-37.
- 892 Mariotti, A. (1983) Atmospheric nitrogen is a reliable standard for natural ¹⁵N abundance
893 measurements. *Nature* **303**, 685–687.
- 894 Mattioli, S. (2011) Family Cervidae, Deer. *Handbook of the Mammals of the World. Vol. 2.*
895 *Hoofed Mammals*. Barcelona: Lynx Edicions.
- 896 Milner, J., Bonenfant, C., Mysterud, A., Gaillard, J.-M., Csányi, S. & Stenseth, N.C. (2006)
897 Temporal and spatial development of red deer harvesting in Europe: Biological and
898 cultural factors. *Journal of Applied Ecology*, **43**, 721-734.
- 899 Michelsen, A., Schmidt, I. K., Jonasson, S., Quarmby, C., & Sleep, D. (1996). Leaf ¹⁵N
900 abundance of subarctic plants provides field evidence that ericoid, ectomycorrhizal
901 and non-and arbuscular mycorrhizal species access different sources of soil nitrogen.
902 *Oecologia*, **105**(1), 53–63.
- 903 Michelsen, A., Quarmby, C., Sleep, D., & Jonasson, S. (1998). Vascular plant ¹⁵N natural
904 abundance in heath and forest tundra ecosystems is closely correlated with presence
905 and type of mycorrhizal fungi in roots. *Oecologia*, **115**(3), 406–418.

- 906 Meiri, M., Lister, A.M., Higham, T.F., Stewart, J.R., Straus, L.G., Obermaier, H., González
907 Morales, M.R., Marín-Arroyo, A.B. & Barnes, I. (2013) Late-glacial recolonization
908 and phylogeography of European red deer (*Cervus elaphus* L.). *Mol Ecol*, **22**, 4711-
909 22.
- 910 Meiri, M., Kosintsev, P., Conroy, K., Meiri, S., Barnes, I. & Lister, A. (2018) Subspecies
911 dynamics in space and time: A study of the red deer complex using ancient and
912 modern DNA and morphology. *Journal of Biogeography*, **45**, 367-380.
- 913 Misarti, N., Finney, B., Maschner, H. & Wooller, M.J. (2009) Changes in northeast Pacific
914 marine ecosystems over the last 4500 years: evidence from stable isotope analysis of
915 bone collagen from archeological middens. *The Holocene*, **19**, 1139-1151.
- 916 Nadelhoffer, K., Shaver, G., Fry, B., Giblin, A., Johnson, L. & McKane, R. (1996) ¹⁵N natural
917 abundances and N use by tundra plants. *Oecologia*, **107**, 386-394.
- 918 Němec, M., Wacker, L. & Gäggeler, H. (2010) Optimization of the Graphitization Process at
919 Age-1. *Radiocarbon*, **52**, 1380-1393.
- 920 Niedziałkowska, M., Doan, K., Górny, M., Sykut, M., Stefaniak, K., Piotrowska, N.,
921 Jędrzejewska, B., Ridush, B., Pawełczyk, S., Mackiewicz, P., Schmölcke, U.,
922 Kosintsev, P., Makowiecki, D., Charniański, M., Krasnodębski, D., Rannamäe, E.,
923 Saarma, U., Arakelyan, M., Manaseryan, N., Titov, V. V., Hulva, P., Bălăşescu, A.,
924 Fyfe, R., Woodbridge, J., Trantalidou, K., Dimitrijević, V., Kovalchuk, O.,
925 Wilczyński, J., Obadã, T., Lipecki, G., Arabey, A. & Stanković, A. (2021) Winter
926 temperature and forest cover have shaped red deer distribution in Europe and the Ural
927 Mountains since the Late Pleistocene. *Journal of Biogeography*, **48**, 147-159.
- 928 Ohtsu, Ayano & Takatsuki, Seiki. (2021). Diets and habitat selection of takhi and red deer in
929 Hustai National Park, Mongolia. *Wildlife Biology*. **2021**(1). 10.2981/wlb.00749.
- 930 Piotrowska, N. & Goslar, T. (2002) Preparation of Bone Samples in the Gliwice Radiocarbon
931 Laboratory for AMS Radiocarbon Dating. *Isotopes in Environmental and Health
932 Studies*, **38**, 267-275.
- 933 Pitra, C., Fickel, J., Meijaard, E. & Groves, C. (2004) Evolution and phylogeny of old world
934 deer. *Molecular Phylogenetics and Evolution*, **33**, 880-895.
- 935 Puhe, J. & Ulrich, B. (2001) Global Climate Change and Human Impacts on Forest
936 Ecosystems. *Ecological Studies Series* Vol. 143. Berlin, Heidelberg: Springer.
- 937 Pyankov, V. I., Ziegler, H., Akhiani, H., Deigele, C., & Luetge, U. (2010). European plants
938 with C4 photosynthesis: geographical and taxonomic distribution and relations to
939 climate parameters. *Botanical Journal of the Linnean Society*, **163**(3), 283-304.
- 940 Queiros, J., Acevedo, P., Santos, J.P., Barasona, J., Beltrán-Beck, B., González-Barrio, D.,
941 Armenteros, J., Diez-Delgado, I., Boadella, M., Ruiz-Fons, F., Vicente, J., de la
942 Fuente, J., Gortázar, C., Searle, J. & Alves, P. (2019) Red deer in Iberia: Molecular
943 ecological studies in a southern refugium and inferences on European postglacial
944 colonization history. *PLOS ONE*, **14**, e0210282.
- 945 R Development Core Team (2018) *R: A language and environment for statistical computing*.
946 Vienna: R Foundation for Statistical Computing.
- 947 Reade, H., Tripp, J.A., Charlton, S., Grimm, S., Leesch, D., Müller, W., Sayle, K.L.,
948 Fensome, A., Higham, T.F.G., Barnes, I., Stevens, R. E. (2020) Deglacial landscapes
949 and the Late Upper Palaeolithic of Switzerland. *Quaternary Science Reviews* **239**,
950 106372.
- 951 Reimer, P.J., Austin, W.E.N., Bard, E., Bayliss, A., Blackwell, P.G., Bronk Ramsey, C.,
952 Butzin, M., Cheng, H., Edwards, R.L., Friedrich, M., Grootes, P.M., Guilderson, T.P.,
953 Hajdas, I., Heaton, T.J., Hogg, A.G., Hughen, K.A., Kromer, B., Manning, S.W.,
954 Muscheler, R., Palmer, J.G., Pearson, C., van der Plicht, J., Reimer, R.W., Richards,
955 D.A., Scott, E.M., Southon, J.R., Turney, C.S.M., Wacker, L., Adolphi, F., Büntgen,

- 956 U., Capano, M., Fahrni, S.M., Fogtmann-Schulz, A., Friedrich, R., Köhler, P., Kudsk,
957 S., Miyake, F., Olsen, J., Reinig, F., Sakamoto, M., Sookdeo, A. & Talamo, S. (2020)
958 The IntCal20 Northern Hemisphere Radiocarbon Age Calibration Curve (0–55 cal
959 kBP). *Radiocarbon*, **62**, 725-757.
- 960 Roberts, N., Fyfe, R.M., Woodbridge, J., Gaillard, M.J., Davis, B.A.S., Kaplan, J.O.,
961 Marquer, L., Mazier, F., Nielsen, A.B., Sugita, S., Trondman, A.K. & Leydet, M.
962 (2018) Europe's lost forests: a pollen-based synthesis for the last 11,000 years.
963 *Scientific Reports*, **8**, 716.
- 964 Rofes, J., García-Ibaibarriaga, N., Aguirre, M., Martínez-García, B., Ortega, L., Zuluaga, M.,
965 Bailón, S., Alonso-Olazabal, A., Castañón, J. & Murelaga, M. (2015) Combining
966 Small-Vertebrate, Marine and Stable-Isotope Data to Reconstruct Past Environments.
967 *Scientific Reports*, **5**, 14219.
- 968 Saarinen, J., Eronen, J., Fortelius, M. & Lister, A. (2016) Patterns of diet and body mass of
969 large ungulates from the Pleistocene of Western Europe, and their relation to
970 vegetation. *Paleontologia Electronica*, **19**, 10.26879/443.
- 971 Sah, S. & Brumme, R. (2003) Natural ¹⁵N abundance in two nitrogen saturated forest
972 ecosystems at Solling, Germany. *Journal of Forest Science*, **49**(11), 10.17221/4794-
973 JFS.
- 974 Skog, A., Zachos, F.E., Rueness, E.K., Feulner, P.G.D., Mysterud, A., Langvatn, R.,
975 Lorenzini, R., Hmwe, S.S., Lehoczy, I., Hartl, G.B., Stenseth, N.C. & Jakobsen, K.S.
976 (2009) Phylogeography of red deer (*Cervus elaphus*) in Europe. *Journal of*
977 *Biogeography*, **36**, 66-77.
- 978 Smith, R.S. & Gregory, J. (2012) The last glacial cycle: transient simulations with an
979 AOGCM. *Climate Dynamics*, **38**, 1545-1559.
- 980 Sommer, R.S., Zachos, F.E., Street, M., Jöris, O., Skog, A. & Benecke, N. (2008) Late
981 Quaternary distribution dynamics and phylogeography of the red deer (*Cervus*
982 *elaphus*) in Europe. *Quaternary Science Reviews*, **27**, 714-733.
- 983 Sommer, R.S. & Zachos, F.E. (2009) Fossil evidence and phylogeography of temperate
984 species: 'glacial refugia' and post-glacial recolonization. *Journal of Biogeography*, **36**,
985 2013-2020.
- 986 Sommer, R.S. (2020) Late Pleistocene and Holocene History of Mammals in Europe. In K.
987 Hackländer, & F. Zachos (Eds.), *Mammals of Europe - Past, Present, and Future.*
988 *Handbook of the Mammals of Europe* (pp. 83-98). Cham: Springer.
- 989 Stankovic, A., Doan, K., Mackiewicz, P., Ridush, B., Baca, M., Gromadka, R., Socha, P.,
990 Węgleński, P., Nadachowski, A. & Stefaniak, K. (2011) First ancient DNA sequences
991 of the Late Pleistocene red deer (*Cervus elaphus*) from the Crimea, Ukraine.
992 *Quaternary International*, **245**, 262-267.
- 993 Stefaniak, K. (2015) *Neogene and Quaternary Cervidae from Poland*. Institute of Systematics
994 and Evolution of Animals Polish Academy of Sciences.
- 995 Stepanova, V.V. (2010) Expansion of geographic range of red deer in Yakutia. *Russian*
996 *Journal of Biological Invasions*, **1**, 30-36.
- 997 Stevens, R. E., & Hedges, R. E. (2004). Carbon and nitrogen stable isotope analysis of
998 northwest European horse bone and tooth collagen, 40,000 BP–present:
999 Palaeoclimatic interpretations. *Quaternary Science Reviews*, **23**(7-8), 977-991.
- 1000 Stevens, R. E., Lister, A. M., & Hedges, R. E. M. (2006). Predicting Diet, Trophic Level and
1001 Palaeoecology from Bone Stable Isotope Analysis: A Comparative Study of Five Red
1002 Deer Populations. *Oecologia*, **149**(1), 12–21.
- 1003 Stevens, R. E., Hermoso-Buxán, X. L., Marín-Arroyo, A. B., Gonzalez-Morales, M. R., &
1004 Straus, L. G. (2014). Investigation of Late Pleistocene and Early Holocene
1005 palaeoenvironmental change at El Mirón cave (Cantabria, Spain): Insights from

- 1006 carbon and nitrogen isotope analyses of red deer. *Palaeogeography,*
1007 *Palaeoclimatology, Palaeoecology*, **414**, 46-60.
- 1008 Sykut, M., Pawełczyk, S., Borowik, T., Pokorny, B., Flajšman, K. & Niedziałkowska, M.
1009 (2020) Intraindividual and interpopulation variability in carbon and nitrogen stable
1010 isotope ratios of bone collagen in the modern red deer (*Cervus elaphus*). *Journal of*
1011 *Archaeological Science: Reports*, **34**, 102669.
- 1012 Sykut, M., Pawełczyk, S., Borowik, T., Pokorny, B., Flajšman, K., Hunink, T. &
1013 Niedziałkowska, M. (2021) Environmental factors shaping stable isotope signatures of
1014 modern red deer (*Cervus elaphus*) inhabiting various habitats. *PLoS One*, **16**,
1015 e0255398.
- 1016 Tieszen, L.L. (1991) Natural variations in the carbon isotope values of plants: Implications for
1017 archaeology, ecology, and paleoecology. *Journal of Archaeological Science*, **18**, 227-
1018 248.
- 1019 Van der Merwe, N. J., & Medina, E. (1991). The canopy effect, carbon isotope ratios and
1020 foodwebs in Amazonia. *Journal of archaeological science*, **18**(3), 249-259.
- 1021 Van der Made, J., Stefaniak, K. & Marciszak, A. (2014) The Polish fossil record of the wolf
1022 *Canis* and the deer *Alces*, *Capreolus*, *Megaloceros*, *Dama* and *Cervus* in an
1023 evolutionary perspective. *Quaternary International*, **326-327**, 406-430.
- 1024 Van der Made, J. & Dimitrijević, V. (2015) *Eucladoceros montenegrensis* n. sp. and other
1025 *Cervidae* from the Lower Pleistocene of Trlica (Montenegro). *Quaternary*
1026 *International*, **389**, 90-118.
- 1027 Van Klinken, G., Plicht, H. & Hedges, R. (1994) Bond $^{13}\text{C}/^{12}\text{C}$ ratios reflect (palaeo-) climatic
1028 variations. *Geophysical Research Letters*, **21**, 445-448.
- 1029 Wacker, L., Němec, M. & Bourquin, J. (2010) A revolutionary graphitisation system: Fully
1030 automated, compact and simple. *Nuclear Instruments and Methods in Physics*
1031 *Research Section B: Beam Interactions with Materials and Atoms*, **268**, 931-934.
- 1032 Wood, S. (2017) *Generalized Additive Models: An Introduction With R*. Boca Raton, FL:
1033 Chapman and Hall/CRC.
- 1034 Woodbridge, J., Roberts, N. & Fyfe, R. (2018) Pan-Mediterranean Holocene vegetation and
1035 land-cover dynamics from synthesized pollen data. *Journal of Biogeography*, **45**,
1036 2159-2174.
- 1037 Zanon, M., Davis, B.A.S., Marquer, L., Brewer, S. & Kaplan, J.O. (2018) European Forest
1038 Cover During the Past 12,000 Years: A Palynological Reconstruction Based on
1039 Modern Analogs and Remote Sensing. *Frontiers in plant science*, **9**, 253.
- 1040 Zech, M., Bimüller, C., Hemp, A., Samimi, C., Broesike, C., Hörold, C. & Zech, W. (2011)
1041 Human and climate impact on ^{15}N natural abundance of plants and soils in high-
1042 mountain ecosystems: a short review and two examples from the Eastern Pamirs and
1043 Mt. Kilimanjaro. *Isotopes in Environmental and Health Studies*, **47**, 286-296.
- 1044 Zhu, Y., Siegwolf, R.T.W., Durka, W. & Körner, C. (2010) Phylogenetically balanced
1045 evidence for structural and carbon isotope responses in plants along elevational
1046 gradients. *Oecologia*, **162**, 853-863.
- 1047 Zoppi, U. (2010) Radiocarbon AMS Data Analysis: From Measured Isotopic Ratios to ^{14}C
1048 Concentrations. *Radiocarbon*, **52**, 165-170.
- 1049 Zoppi, U., Crye, J., Song, Q. & Arjomand, A. (2007) Performance Evaluation of the New
1050 AMS System at Accium BioSciences. *Radiocarbon*, **49**, 171-180.

1051
1052
1053

Supplementary material

1054 **Supplementary material 1**

1055 Table S1 Database of stable isotopic values and direct radiocarbon dates of red deer *s. l.*
1056 samples and the climatic and environmental data determined for their localities and analysed
1057 in the frame of this study.

1058 Table S2 Stable isotopic data and radiocarbon dates of red deer samples from different sites in
1059 Europe obtained from the literature sources.

1060 Table S3 Results of isotopic analyses ($\delta^{13}\text{C}$, $\delta^{15}\text{N}$) on bone collagen of modern red deer,
1061 composition of the collagen (carbon/nitrogen ratio, percentage of nitrogen and carbon in a
1062 sample), year of death of sampled red deer individual, percentage of forest cover and open
1063 area calculated in buffers around the sample sites (see Sykut *et al.*, 2021 for more details).
1064 Study sites with abbreviated country name: PL-Poland, NL-Netherlands, UK-United
1065 Kingdom, SI-Slovenia,* samples with $\delta^{13}\text{C}$ and $\delta^{15}\text{N}$ values recalculated by the formulas
1066 described in the (Sykut *et al.*, 2020); $\delta^{13}\text{C}$ corr: $\delta^{13}\text{C}$ values corrected for the shift in $\delta^{13}\text{C}$
1067 values (corr atm) caused by anthropogenic CO_2 emissions by the formula proposed by (Feng,
1068 1998).

1069 Table S4 List of the Holocene red deer samples, genetic, climatic and environmental data
1070 used in the Normal linear models (NLM). Abbreviations as in Tab. S1.

1071 **Supplementary material 2**

1072 Table S5 Pairwise correlation matrix of the following parameters: percentage of forest cover,
1073 percentage of open area, mean annual temperature, mean July temperature, mean January
1074 temperature, altitude, annual precipitation in each of the study sites, where the red deer
1075 Holocene fossils ($n = 39$, Tab. S4) were recorded and dated for certain time periods.
1076 Significant assays ($P \leq 0.05$) are given in bold.

1077 Table S6. Parameters of regression between $\delta^{13}\text{C}$ and $\delta^{15}\text{N}$ values and the median of
1078 calibrated age BP of samples calculated in various localities of European red deer populations
1079 presented in Fig. S6. Significant assays ($P \leq 0.05$) are given in bold.

1080 Fig. S1 Geographic distribution of modern red deer samples used in this study (n = 49) and
1081 published in Sykut *et al.* (2021).

1082 Fig. S2 Stable carbon ($\delta^{13}\text{C}$) and nitrogen ($\delta^{15}\text{N}$) isotope signatures of red deer *s.l.* from
1083 different habitats into two time periods before the LGM (47 857 – 26 813 cal BP) (upper
1084 panel) and after LGM (9508 – 189 cal BP) (lower panel). Wapiti biome categories: Forest -
1085 deciduous taiga or montane forest; Open - shrub or steppe tundra; Mixed - xerophytic shrub
1086 or sclerophyll woodland. The regression parameters were calculated for the wapiti samples
1087 only, including all *C. canadensis* samples and separately for wapiti inhabiting forest (F) and
1088 open (O) biomes. Wapiti from mixed and desert biomes were not included in the statistical
1089 analyses. Red deer biome categories: Forest – deciduous montane or coniferous forest, Mixed
1090 - sclerophyll woodland.

1091

1092 Fig. S3 Stable carbon ($\delta^{13}\text{C}$) and nitrogen ($\delta^{15}\text{N}$) isotope signatures of red deer *s.l.* from
1093 different mitochondrial lineages and haplogroups into two time periods before the LGM (47
1094 857 – 26 813 cal BP) (upper panel) and after LGM (9508 – 189 cal BP) (lower panel).

1095